Polynomial splines over locally refined box-partitions

Article *in* Computer Aided Geometric Design · March 2013

DOI: 10.1016/j.cagd.2012.12.005

Computer Aided Geometric Design 30 (2013) 331–356

Contents lists available at SciVerse ScienceDirect

Computer Aided Geometric Design

www.elsevier.com/locate/cagd

Polynomial splines over locally refined box-partitions ☆

Tor Dokken [a,2,3], Tom Lyche [b,*,1], Kjell Fredrik Pettersen [a]

[a] SINTEF, PO Box 124 Blindern, 0314 Oslo, Norway
[b] CMA, University of Oslo, PO Box 1053 Blindern, 0316 Oslo, Norway

ARTICLE INFO

Article history:
Received 23 February 2012
Received in revised form 20 December 2012
Accepted 22 December 2012
Available online 25 January 2013

Keywords:
Box-partitions
LR-meshes
Dimension of spline spaces
Locally refined tensor product B-splines
Isogeometric analysis

ABSTRACT

We address progressive local refinement of splines defined on axes parallel box-partitions and corresponding box-meshes in any space dimension. The refinement is specified by a sequence of mesh-rectangles (axes parallel hyperrectangles) in the mesh defining the spline spaces. In the 2-variate case a mesh-rectangle is a knotline segment. When starting from a tensor-mesh this refinement process builds what we denote an LR-mesh, a special instance of a box-mesh. On the LR-mesh we obtain a collection of hierarchically scaled B-splines, denoted LR B-splines, that forms a nonnegative partition of unity and spans the complete piecewise polynomial space on the mesh when the mesh construction follows certain simple rules. The dimensionality of the spline space can be determined using some recent dimension formulas.

1. Introduction

Splines are used as a tool in a wide range of applications both in academia and industry for the representation of functions and parametric curves, surfaces and solids in one, two or more variables. Although a number of alternative spline bases exist, B-Splines or NonUniform Rational B-splines (NURBS) are most often used in the univariate case. Similarly, multivariate splines spaces on quadrilateral and hexagonal meshes are most often represented using the tensor-products of univariate B-splines or NURBS. The popularity of tensor-product B-splines stems from a number of reasons:

- Efficient and numerically stable algorithms for knot insertion, degree raising and evaluation of values and derivatives.
- Coefficients have a geometric interpretation as corners in a control polygon that mimics the shape of the spline.
- NURBS is the standardized representation for rational splines in the STEP standard,[4] used in Computer Aided Design.

In this paper we introduce the concept of Locally Refined Splines (LR-splines) that breaks the tensor-product mesh structure by introducing local refinements. LR-splines are related to hierarchical B-splines introduced by Forsey and Bartels (1988). The challenges of linear independence of hierarchical B-splines were solved in the PhD thesis of Kraft (1998), and have recently been further elaborated in Vuong et al. (2011). For recent results on approximation properties see Babenko et al. (2011). T-splines were introduced by Sederberg et al. (2003, 2004) as a way to model surfaces using fewer control points

☆ This paper has been recommended for acceptance by H. Prautzsch.
* Corresponding author.
E-mail addresses: tor.dokken@sintef.no (T. Dokken), tom@ifi.uio.no (T. Lyche), KjellFredrik.Pettersen@sintef.no (K.F. Pettersen).
[1] We like to thank the referees for comments improving the presentation.
[2] The research leading to these results are partly funded by the European Community's Seventh Framework Programme FP7/2007-2013 under grant agreement No. 284981 (TERRIFIC).
[3] We thank Kjetil Johannesen for Fig. 15 and Odd Andersen for Fig. 17.
[4] ISO 10303 – Automation systems and integration – Product data representation and exchange.

0167-8396/$ – see front matter
http://dx.doi.org/10.1016/j.cagd.2012.12.005

than hierarchical B-splines. PHT-splines were introduced in Deng et al. (2008) as an alternative C^1 bi-cubic approach to local refinement. Spline spaces over partitions combining triangles and rectangles were addressed in Schumaker and Wang (2011, 2012). A basis is constructed using the concept of minimal determining sets.

The current interest in spline refinement was triggered by the introduction of isogeometric analysis by T.J.R. Hughes et al. (2009, 2005). In isogeometric analysis traditional Finite Elements are replaced by tensor-product NURBS. Some of the advantages are accurate shape representation for analysis, easy use of higher order smoothness, and simplified design optimization by replacing remeshing by model refinement. However, traditional tensor-product splines lack local refinement (Dokken et al., 2009). Consequently spline representation such as T-splines, hierarchical B-splines and LR B-splines have much to contribute for practical deployment of isogeometric analysis in science and industry.

The concepts of box-partitions, box-meshes and LR-meshes are addressed in Section 2, while the definition of LR B-splines over LR-meshes is considered in Section 3. Section 4 addresses the resulting spline spaces and their dimensions. The spanning properties of the LR B-splines is the topic of Section 5. How to ensure that the LR B-splines are linearly independent is discussed in Section 6. In Section 7 partition of unity and convex hull properties of LR B-splines are presented. Then in Section 8 we discuss how LR B-splines can be refined through a 3D vertex mesh in a similar way as T-splines, or through a projection of the LR-mesh on to the 3D surface.

1.1. B-splines

We end this introduction by recalling some properties of B-splines that are needed.

Definition 1.1. On a nondecreasing sequence $\boldsymbol{y} = (y_1, y_2, \ldots, y_{p+2})$ we define a B-spline $B[\boldsymbol{y}] : \mathbb{R} \to \mathbb{R}$ of degree $p \geqslant 0$ recursively by

$$B[\boldsymbol{y}](x) := \frac{x - y_1}{y_{p+1} - y_1} B[y_1, \ldots, y_{p+1}](x) + \frac{y_{p+2} - x}{y_{p+2} - y_2} B[y_2, \ldots, y_{p+2}](x), \tag{1}$$

starting with

$$B[y_i, y_{i+1}](x) := \begin{cases} 1; & \text{if } y_i \leqslant x < y_{i+1}; \\ 0; & \text{otherwise}, \end{cases} \qquad i = 1, \ldots, p+1.$$

We define $B[\boldsymbol{y}] \equiv 0$ if $y_{p+2} = y_1$ and in (1) terms with zero denominator are defined to be zero.

Suppose $y_1 < y_{p+2}$. We recall that $B[\boldsymbol{y}]$ is a piecewise polynomial of degree p on $\boldsymbol{y}$ with support $[y_1, y_{p+2}]$. Moreover, $0 \leqslant B[\boldsymbol{y}](x) \leqslant 1$ for $x \in \mathbb{R}$ and if

$$y_1 \leqslant y_2 \leqslant \cdots \leqslant y_{p+2} = \eta_1^{[m_1]} < \cdots < \eta_l^{[m_l]}, \tag{2}$$

then $B[\boldsymbol{y}] \in C^{p-m_j}$ but not in C^{p-m_j+1} at η_j, $j = 1, \ldots, l$. Here $\eta_1, \ldots, \eta_l$ are the distinct members among the components of $\boldsymbol{y}$, and $\eta_j^{[m_j]}$ means that η_j is repeated m_j times, $j = 1, \ldots, l$. For each j the integer $m_j = m(\eta_j)$ is called the **multiplicity** of η_j in $\boldsymbol{y}$. We define the **multiplicity function** $m_B : \mathbb{R} \to \mathbb{N} \cup \{0\}$ by

$$m_B(t) := \begin{cases} m(\eta_j), & \text{if } t = \eta_j, \text{ for some } j, \text{ with } 1 \leqslant j \leqslant l, \\ 0, & \text{otherwise}. \end{cases} \tag{3}$$

For more properties of B-splines we refer to Schumaker (2007).

Suppose we insert a knot $z \in (y_1, y_{p+2})$. We obtain two new local knot vectors $\boldsymbol{y}_1 := R(\boldsymbol{y}, z, 1)$ and $\boldsymbol{y}_2 := R(\boldsymbol{y}, z, 2)$, where

$$R(\boldsymbol{y}, z, 1) = (z_1, \ldots, z_{p+2}), \qquad R(\boldsymbol{y}, z, 2) = (z_2, \ldots, z_{p+3}), \tag{4}$$

and where $(z_1, \ldots, z_{p+3})$ is the sequence $(y_1, \ldots, y_{p+2}, z)$ rearranged in a nondecreasing order.

Definition 1.2 *(Tensor product B-splines).* Let d be a positive integer, suppose $\boldsymbol{p} = (p_1, \ldots, p_d)$ has nonnegative components, and let $\boldsymbol{y}_k := (y_{k,1}, \ldots, y_{k,p_k+2})$ be nondecreasing sequences $k = 1, \ldots, d$. We define a **tensor-product B-spline** $B[\boldsymbol{Y}] = B[\boldsymbol{y}_1, \ldots, \boldsymbol{y}_d] : \mathbb{R}^d \to \mathbb{R}$ from univariate B-splines $B[\boldsymbol{y}_k]$ by

$$B[\boldsymbol{y}_1, \ldots, \boldsymbol{y}_d](x_1, \ldots, x_d) := \prod_{k=1}^{d} B[\boldsymbol{y}_k](x_k).$$

The **support** of B is given by the Cartesian product

$$\operatorname{supp}(B) := [y_{1,1}, y_{1,p_1+2}] \times \cdots \times [y_{d,1}, y_{d,p_d+2}]. \tag{5}$$

Suppose we insert a knot z in $(y_{k,1}, y_{k,p_k+2})$ for some $1 \leqslant k \leqslant d$. Then

$$B[\boldsymbol{Y}] = \alpha_1 B[\boldsymbol{Y}_1] + \alpha_2 B[\boldsymbol{Y}_2], \tag{6}$$

where

$$\boldsymbol{Y}_s = R_k(\boldsymbol{Y}, z, s) := \big(\boldsymbol{y}_1, \ldots, \boldsymbol{y}_{k-1}, R(\boldsymbol{y}_k, z, s), \boldsymbol{y}_{k+1}, \ldots, \boldsymbol{y}_d\big), \quad s = 1, 2, \tag{7}$$

and

$$\alpha_1 := \begin{cases} 1, & y_{k,p_k+1} \leqslant z < y_{k,p_k+2}, \\ \frac{z - y_{k,1}}{y_{k,p_k+1} - y_{k,1}}, & y_{k,1} < z < y_{k,p_k+1}, \end{cases}$$
$$\alpha_2 := \begin{cases} 1, & y_{k,1} < z \leqslant y_{k,2}, \\ \frac{y_{k,p_k+2} - z}{y_{k,p_k+2} - y_{k,2}}, & y_{k,2} < z < y_{k,p_k+2}. \end{cases} \tag{8}$$

2. Boxes and meshes

In this section we consider partitions defined from boxes and their corresponding meshes.

2.1. Box collections

We start by defining a number of useful concepts.

Definition 2.1. Given an integer $d \geqslant 1$. A **box** in $\mathbb{R}^d$ is a Cartesian product

$$\beta = J_1 \times \cdots \times J_d \subseteq \mathbb{R}^d, \tag{9}$$

where each $J_k = [a_k, b_k]$ with $a_k \leqslant b_k$ is a closed finite interval in $\mathbb{R}$. We also write $\beta = [\boldsymbol{a}, \boldsymbol{b}]$, where $\boldsymbol{a} = (a_1, \ldots, a_d)$, and $\boldsymbol{b} = (b_1, \ldots, b_d)$. The interval J_k is said to be **trivial** if $a_k = b_k$ and **nontrivial** otherwise. The **dimension** of β, denoted $\dim\beta$, is the number of nontrivial intervals J_k in (9). We call β an ℓ-box or an (ℓ, d)-box if $\dim\beta = \ell$. If $\dim\beta = d$ then β is called an **element**, while if $\dim\beta = d-1$, there exists exactly one k such that $J_k = \{a\}$ is trivial. Then β is called a **mesh-rectangle**, a k**-mesh-rectangle** or a (k, a)**-mesh-rectangle**.

Several remarks are in order.

1. We often use Greek letters like α, β, γ for boxes.
2. A mesh-rectangle is part of an axes parallel hyperplane and has codimension one in any space dimension. It is a point for $d = 1$, a line segment for $d = 2$, a rectangle for $d = 3$ and a 3-box for $d = 4$. Moreover for $d = 2$, a k-mesh-rectangle is a vertical line segment for $k = 1$ and a horizontal line segment for $k = 2$.
3. A d-box contains $2^{d-\ell}\binom{d}{\ell}$ ℓ-boxes, $\ell = 0, 1, \ldots, d$.
4. A mesh-rectangle $\gamma = [\boldsymbol{c}, \boldsymbol{e}]$ is called a **face of a** d**-box** $[\boldsymbol{a}, \boldsymbol{b}]$ if $c_k = a_k < b_k = e_k$ for the nontrivial intervals and $c_k = e_k = a_k$ or $c_k = e_k = b_k$ for the trivial one. The union of all faces of a d-box $[\boldsymbol{a}, \boldsymbol{b}]$ is called the **boundary** of the box. The interior of a box β is denoted β^o.

In Fig. 1 we show some examples of these concepts.

Definition 2.2 *(Box partition).* Let $\Omega \subseteq \mathbb{R}^d$ be a d-box in $\mathbb{R}^d$. A finite collection $\mathcal{E}$ of d-boxes in $\mathbb{R}^d$ is said to be a **box partition** of Ω if

1. $\beta_1^o \cap \beta_2^o = \emptyset$ for any $\beta_1, \beta_2 \in \mathcal{E}$ where $\beta_1 \neq \beta_2$.
2. $\bigcup_{\beta \in \mathcal{E}} \beta = \Omega$.

A box partition contains a number of boxes of lower dimension. To formalize we start with the following definition.

Definition 2.3. Given a collection $\mathcal{E}$ of d-boxes and a point $\boldsymbol{q} \in \mathbb{R}^d$ we define $\beta_{\boldsymbol{q}} = \beta_{\boldsymbol{q}}(\mathcal{E})$ as the intersection of all boxes in $\mathcal{E}$ containing $\boldsymbol{q}$

$$\beta_{\boldsymbol{q}}(\mathcal{E}) = \bigcap_{\substack{\beta \in \mathcal{E} \\ \boldsymbol{q} \in \beta}} \beta. \tag{10}$$

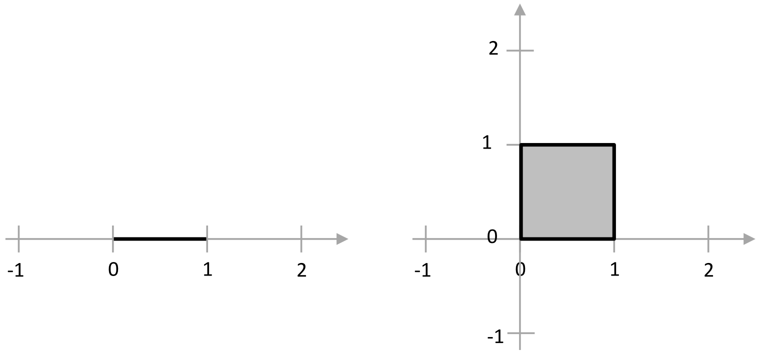

Fig. 1. In the figure to the left there are two $(0,1)$-boxes (points/mesh-rectangles) $\{0\}$ and $\{1\}$, and one $(1,1)$-box (element) $[0,1]$. In the figure to the right there are four $(0,2)$-boxes (points) $(0,0)$, $(1,0)$, $(0,1)$ and $(1,1)$, four $(1,2)$-boxes (line segments/mesh-rectangles) $[0,1]\times\{0\}$, $\{0\}\times[0,1]$, $[0,1]\times\{1\}$, and $\{1\}\times[0,1]$, and one $(2,2)$-box (element) $[0,1]\times[0,1]$.

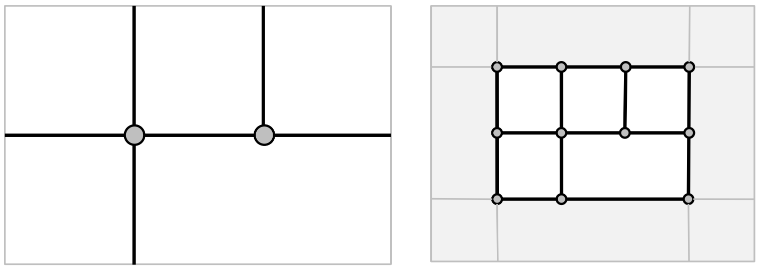

Fig. 2. The figure shows an example of a box partition $\mathcal{E}$ to the left, $\mathcal{E}\cup\Omega^+$ to the right, and their lower dimensional boxes.

Let $\mathcal{E}$ be a box partition of a d-box $\Omega=[\boldsymbol{a},\boldsymbol{b}]\subset\mathbb{R}^d$. In order to also identify lower dimensional ℓ-boxes on the boundaries of $\mathcal{E}$ we define the set

$$\Omega^+=\bigl\{J_1\times\cdots\times J_d\colon\ J_k\in\bigl\{[a_k-1,a_k],[a_k,b_k],[b_k,b_k+1]\bigr\},\ \forall k\bigr\}\setminus\{\Omega\}. \tag{11}$$

If $\mathcal{E}$ is a box partition of Ω, then $\mathcal{E}\cup\Omega^+$ is a box partition of $[a_1-1,b_1+1]\times\cdots\times[a_d-1,b_d+1]$. This is illustrated in Fig. 2.

We can now define sets of boxes of lower dimension in a box partition.

Definition 2.4. Given a box partition $\mathcal{E}$ on a d-box Ω. We define the sets

$$\mathcal{F}(\mathcal{E}):=\bigcup_{\boldsymbol{q}\in\Omega}\bigl\{\beta_q\bigl(\mathcal{E}\cup\Omega^+\bigr)\bigr\}\quad\text{(all boxes of all dimensions)}, \tag{12}$$

$$\mathcal{F}^o(\mathcal{E}):=\bigcup_{\boldsymbol{q}\in\Omega^o}\bigl\{\beta_q(\mathcal{E})\bigr\}\quad\text{(all interior boxes of all dimensions)}, \tag{13}$$

$$\mathcal{F}_\ell(\mathcal{E}):=\bigl\{\beta\in\mathcal{F}(\mathcal{E})\colon\ \dim\beta=\ell\bigr\}\quad\text{for }\ell=0,\dots,d, \tag{14}$$

$$\mathcal{F}^o_\ell(\mathcal{E}):=\bigl\{\beta\in\mathcal{F}^0(\mathcal{E})\colon\ \dim\beta=\ell\bigr\}\quad\text{for }\ell=0,\dots,d. \tag{15}$$

In addition, for $k=1,\dots,d$ we define $\mathcal{F}_{d-1,k}(\mathcal{E})$ as the set of all k-mesh-rectangles in $\mathcal{F}_{d-1}(\mathcal{E})$.

2.2. *Meshes in* $\mathbb{R}^d$

To a box partition there corresponds a mesh consisting of mesh-rectangles. It is natural to assign to each mesh-rectangle γ a multiplicity $\mu=\mu(\gamma)$ and thus provide support for different orders of continuity across different mesh-rectangles.

Definition 2.5 *(Box-mesh and extended box-mesh).* Let $\mathcal{E}$ be a box partition of $\Omega=[\boldsymbol{a},\boldsymbol{b}]\subset\mathbb{R}^d$.

1. The collection $\mathcal{M}=\mathcal{M}(\mathcal{E}):=\mathcal{F}_{d-1}(\mathcal{E})$ of minimal $(d-1)$ boxes is called a **box-mesh** on $[\boldsymbol{a},\boldsymbol{b}]$.
2. If to each $\gamma\in\mathcal{M}$ there is an associated integer $\mu(\gamma)\geqslant 1$, then $(\mathcal{M},\mu)$ is called a **$\boldsymbol{\mu}$-extended box-mesh**, or an **extended box-mesh** when the context allows. Note that $\mu:\mathcal{M}\to\mathbb{N}$ is a function.

3. We define

$$\mathcal{F}(\mathcal{M}) := \mathcal{F}\big(\mathcal{E}(\mathcal{M})\big), \tag{16}$$
$$\mathcal{F}_\ell(\mathcal{M}) := \mathcal{F}_\ell\big(\mathcal{E}(\mathcal{M})\big) \quad \text{for any } \ell = 0, \ldots, d, \tag{17}$$
$$\beta_{\boldsymbol{q}}(\mathcal{M}) := \beta_{\boldsymbol{q}}\big(\mathcal{E}(\mathcal{M})\big) \quad \text{for any } \boldsymbol{q} \in \Omega, \tag{18}$$
$$\mathcal{F}_{d-1,k}(\mathcal{M}) := \mathcal{F}_{d-1,k}\big(\mathcal{E}(\mathcal{M})\big), \tag{19}$$

where $\mathcal{E}(\mathcal{M})$ denotes the unique box partition used to define $\mathcal{M}$.

Note that a box-mesh is a μ-extended box mesh, where $\mu(\gamma) = 1$ for all $\gamma \in \mathcal{M}$. For $d = 2$ an interior vertex in a box-mesh belongs to either 4 or 3 rectangles, known as a cross($+$) or a T($\top$) vertex, respectively. Note that we do not allow L-shaped elements in a box-mesh.

Definition 2.6 *(Tensor-mesh).* Given $d \in \mathbb{N}$ and sequences $(a_{k,1}, \ldots, a_{k,n_k})$ in $\mathbb{R}$ with $a_{k,1} < \cdots < a_{k,n_k}$ for $k = 1, \ldots, d$. The box-mesh $\mathcal{M} := \mathcal{F}_{d-1}(\mathcal{E})$ corresponding to the box-partition

$$\begin{aligned}\mathcal{E} &= \big\{[\boldsymbol{a_i}, \boldsymbol{a_{i+1}}]\colon \boldsymbol{1} \leqslant \boldsymbol{i} \leqslant \boldsymbol{n} - \boldsymbol{1}\big\} \\ &= \big\{[a_{1,i_1}, a_{1,i_1+1}] \times \cdots \times [a_{d,i_d}, a_{d,i_d+1}]\colon 1 \leqslant i_k \leqslant n_k - 1, k = 1, \ldots, d\big\}\end{aligned} \tag{20}$$

is called a **tensor-mesh**.

In general, a tensor-mesh can be constructed from a collection of nondecreasing univariate knot vectors.

Definition 2.7. A **μ-extended tensor-mesh** is a μ-extended box-mesh $(\mathcal{M}, \mu)$ such that $\mathcal{M}$ is a tensor-mesh and $\mu(\gamma) = \mu(\gamma')$ whenever γ and γ' are in the same hyperplane.

Sometimes it is convenient to extend a box-mesh to a tensor-mesh.

Definition 2.8. Let $\mathcal{M}$ and $(\mathcal{M}, \mu)$ be a box-mesh and a μ-extended box-mesh, respectively. We define the **tensor-mesh expansion** $\mathcal{M}^T$ **of** $\mathcal{M}$ as the smallest tensor-mesh containing $\mathcal{M}$. The μ^T **extension of** μ **with respect to** $\mathcal{M}$, $\mu^T : \mathcal{M}^T \to \mathbb{N} \cup \{0\}$, is defined by

$$\mu^T(\beta) := \begin{cases} \mu(\gamma), & \text{if } \beta \subseteq \gamma \in \mathcal{M}, \\ 0, & \text{if } \beta \nsubseteq \gamma, \text{ all } \gamma \in \mathcal{M}. \end{cases}$$

We call $(\mathcal{M}^T, \mu^T)$ the **μ-extended tensor-mesh expansion** of $(\mathcal{M}, \mu)$.

Fig. 3 shows a box mesh, an example of a μ-extension, and the corresponding extended tensor-mesh expansion.

LR-meshes are constructed by successive refinement of box-meshes such that in each refinement at least one d-box is split in two by a mesh-rectangle γ, or by increasing multiplicity as described in the following definitions.

Definition 2.9 *(Splits).* Given a mesh-rectangle γ and a d-box β in $\mathbb{R}^d$. We say that γ **splits** β if $\beta \setminus \gamma$ is not connected. We say that γ is a **minimal split** of β if it splits β and $\gamma \subseteq \beta$. If γ splits β, $\beta \setminus \gamma$ has two components β_1 and β_2 each being connected. We define $X_{\beta,\gamma} := \{\bar{\beta}_1, \bar{\beta}_2\}$, where $\bar{\beta}_j$ is the closure of β_j, $j = 1, 2$.

Given a box partition $\mathcal{E}$ of a d-box Ω and a mesh-rectangle γ in $\mathbb{R}^d$. We say that γ **splits** $\mathcal{E}$ if γ is a finite union $\bigcup_i \gamma_i$ of mesh-rectangles such that each γ_i is either a minimal split of a box in $\mathcal{E}$ or is a mesh-rectangle in $\mathcal{M}(\mathcal{E})$.

Definition 2.10. Given a box partition $\mathcal{E}$ of a d-box Ω and a mesh-rectangle γ in $\mathbb{R}^d$ that splits $\mathcal{E}$. Let $\mathcal{E}_1$ be the set of all boxes in $\mathcal{E}$ that are split by γ, and $\mathcal{E}_2 = \mathcal{E} \setminus \mathcal{E}_1$. We define

$$\mathcal{E} + \gamma := \mathcal{E}_2 \cup \bigg(\bigcup_{\beta \in \mathcal{E}_1} X_{\beta,\gamma}\bigg), \tag{21}$$

which is another box partition of Ω. If $\mathcal{M} = \mathcal{F}_{d-1}(\mathcal{E})$ we define

$$\mathcal{M} + \gamma := \mathcal{F}_{d-1}(\mathcal{E} + \gamma). \tag{22}$$

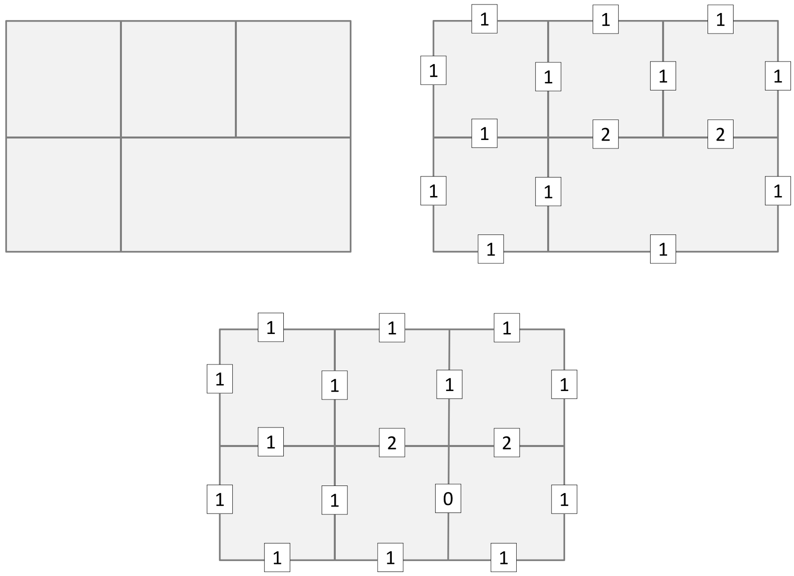

Fig. 3. A box-mesh, an example of a μ-extension, and its tensor-mesh expansion.

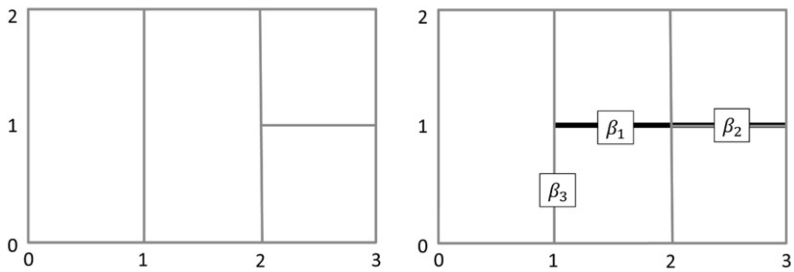

Fig. 4. An illustration of the three cases in Definition 2.11. The mesh-rectangle $\gamma = [1,3] \times \{1\}$ is inserted. The mesh-rectangle $\beta_1 = [1,2] \times \{1\} \subseteq \gamma$ does not exist from before and is assigned multiplicity 1. On the other hand $\beta_2 = [2,3] \times \{1\} \subseteq \gamma$ is already present and the multiplicity is increased by one. The third case is illustrated by $\beta_3 = \{1\} \times [0,1]$ that is a subset of the mesh-rectangle $\{1\} \times [0,2]$ that existed before γ was inserted but that is not a subset of γ.

Definition 2.11 *(Extended box partition split).* Let $(\mathcal{M}, \mu)$ be a μ-extended box-mesh in $\mathbb{R}^d$ and let γ be a mesh-rectangle. The μ-extension μ_γ of a mesh-rectangle $\beta \in \mathcal{M} + \gamma$ is defined as follows:

$$\mu_\gamma(\beta) := \begin{cases} 1 & \text{if } \beta \nsubseteq \beta' \text{ for all } \beta' \in \mathcal{M}, \\ \mu(\beta') + 1 & \text{if } \beta \subseteq \beta' \subseteq \gamma \text{ for } \beta' \in \mathcal{M}, \\ \mu(\beta') & \text{if } \beta \subseteq \beta' \nsubseteq \gamma \text{ for } \beta' \in \mathcal{M}. \end{cases} \tag{23}$$

We say that γ is a **constant split** of $(\mathcal{M}, \mu)$ of **multiplicity** $\mu(\gamma)$ if $\mu(\gamma) := \mu_\gamma(\beta)$ is the same for all $\beta \in \mathcal{M} + \gamma$ with $\beta \subseteq \gamma$.

An illustration of Definition 2.11 is shown in Fig. 4.
We can now give a recursive definition of an LR-mesh.

Definition 2.12. A **μ-extended LR-mesh** is a μ-extended box-mesh $(\mathcal{M}, \mu)$ where either

1. $(\mathcal{M}, \mu)$ is a μ-extended tensor-mesh or
2. $(\mathcal{M}, \mu) = (\tilde{\mathcal{M}} + \gamma, \tilde{\mu}_\gamma)$ where $(\tilde{\mathcal{M}}, \tilde{\mu})$ is a μ-extended LR-mesh and γ is a constant split of $(\tilde{\mathcal{M}}, \tilde{\mu})$.

If $(\mathcal{M}, \mu)$ is a μ-extended LR-mesh then $\mathcal{M}$ is called an **LR-mesh**.

A box-mesh, and an LR-mesh are shown in Fig. 5. The box-mesh on the left is not an LR-mesh. Indeed, $\mathcal{M}_1$ is the boundary of the rectangle, and there is no way we can insert one of the line segments so that it splits the rectangle in two elements. The construction of a trivariate LR-mesh is shown in Fig. 6.

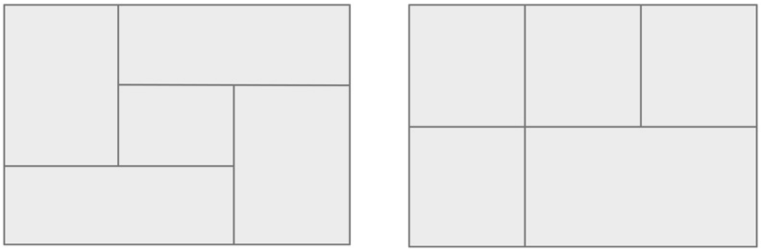

Fig. 5. A box-mesh (left) and an LR-mesh (right).

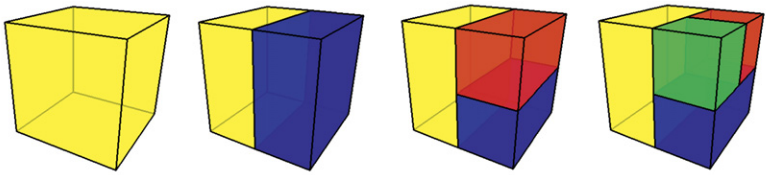

Fig. 6. Construction of a 3-dimensional LR-mesh in parameter space.

It would be interesting to decide if a given box-mesh is an LR-mesh. To check this we do not know any other way than using the steps of Definition 2.12.

3. LR B-splines

In Definition 2.12 the LR-mesh was defined recursively, and we will now define LR B-splines following a similar recursive approach.

3.1. Definition of LR B-splines

To define LR B-splines we need the concept of minimal support. To do this we need tools for comparing and measuring minimal multiplicity of points in a set with respect to a μ-extended box-mesh.

Definition 3.1. Given a μ-extended box-mesh $(\mathcal{M}, \mu)$. For any point $\boldsymbol{q} \in \mathbb{R}^d$, any $X \subset \mathbb{R}^d$, and any $k = 1, \ldots, d$, we define

$$\mu_k(\boldsymbol{q}) = \max\bigl(\{0\} \cup \bigl\{\mu(\gamma)\colon \boldsymbol{q} \in \gamma \in \mathcal{F}_{d-1,k}(\mathcal{M})\bigr\}\bigr), \tag{24}$$

$$\nu_k(X) = \inf\bigl\{\mu_k\bigl(\{\boldsymbol{q}\}\bigr)\colon \boldsymbol{q} \in X\bigr\}. \tag{25}$$

See Fig. 7 for some examples.

Definition 3.2. The tensor-product B-spline given by $B(\boldsymbol{x}) = B(x_1, \ldots, x_d) = B_1(x_1) \cdots B_d(x_d)$, has **support** in the μ-extended box-mesh $(\mathcal{M}, \mu)$ if

$$m_{B_k}(t) \leqslant \nu_k\bigl(\operatorname{supp}(B) \cap \phi_{k,t}\bigr) \tag{26}$$

for every $k = 1, \ldots, d$ and every $t \in \operatorname{supp}(B_k)$. Here $m_{B_k}(t)$ is the knot multiplicity of B_k at t, (see (3)), and $\phi_{k,t}$ is the axes parallel hyperplane $\phi_{k,t} = \mathbb{R}^{k-1} \times \{t\} \times \mathbb{R}^{d-k}$.

B has **minimal support** in $(\mathcal{M}, \mu)$ if it has support in $(\mathcal{M}, \mu)$, and in addition

$$m_{B_k}(t) = \nu_k\bigl(\operatorname{supp}(B) \cap \phi_{k,t}\bigr), \tag{27}$$

for every $k = 1, \ldots, d$ and every $t \in \operatorname{supp}(B_k)^o$.

Definition 3.2 is illustrated in Fig. 8.

We now have all the concepts we need to define an LR B-spline.

Definition 3.3 *(LR B-splines).* Let $(\mathcal{M}, \mu)$ be a μ-extended LR-mesh in $\mathbb{R}^d$. A function $B : \mathbb{R}^d \to \mathbb{R}$ is called an **LR B-spline** on $(\mathcal{M}, \mu)$ if B is a tensor-product B-spline with minimal support in $(\mathcal{M}, \mu)$.

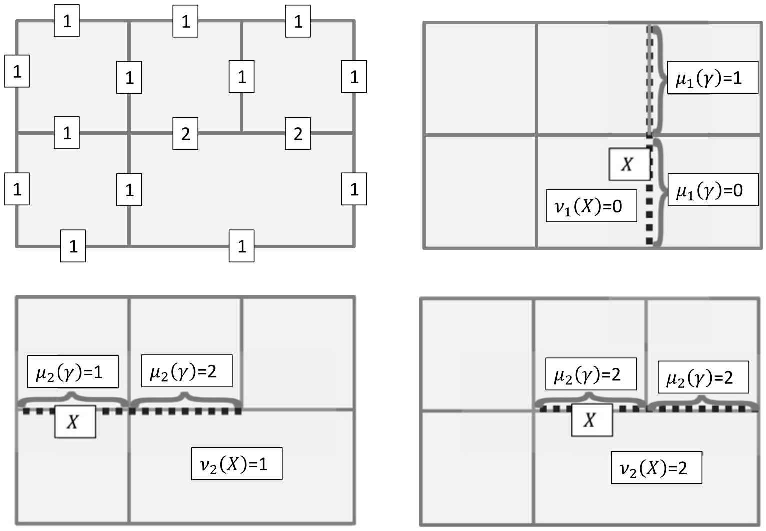

Fig. 7. A μ-extended box-mesh, and three examples of sets X (dotted) and the resulting value of $\nu_k(X)$.

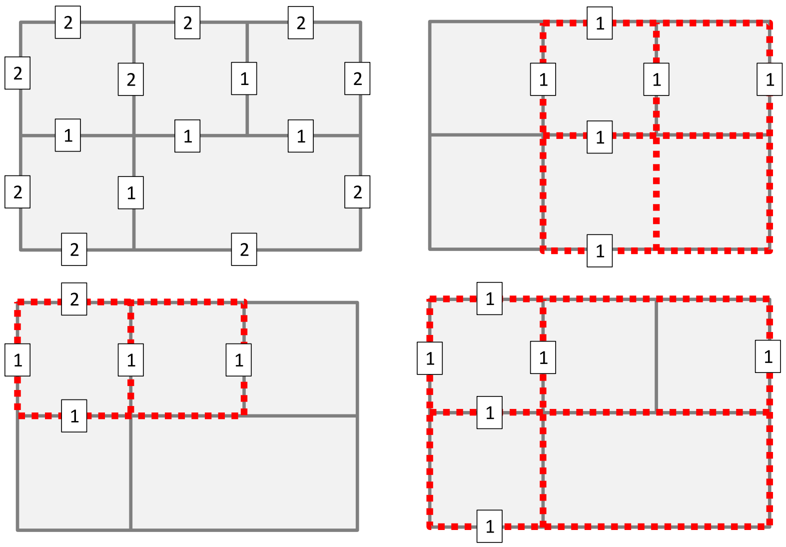

Fig. 8. A μ-extended box-mesh $\mathcal{M}$ at the top left, and 3 examples of bilinear B-splines and their relation to $\mathcal{M}$. The B-spline indicated by the knotline multiplicities at the top to the right does not have support in $\mathcal{M}$ since a part of a knotline of the B-spline is not present in $\mathcal{M}$. The two examples below have support in $\mathcal{M}$, but only the B-spline to the right has minimal support in $\mathcal{M}$. In the B-spline to the left the internal vertical knotline has lower multiplicity than the corresponding mesh-rectangle in $\mathcal{M}$.

3.2. B-splines on an LR-mesh

Given a μ-extended LR-mesh $(\mathcal{M},\mu)$ and a multi-degree $\boldsymbol{p}=(p_1,\dots,p_d)$ we now define a collection $\mathcal{B}$ of LR B-splines of degree $\boldsymbol{p}$ on $(\mathcal{M},\mu)$. Recall that $(\mathcal{M},\mu)$ is defined as a sequence of μ-extended LR-meshes $(\mathcal{M}_1,\mu_1),\dots,(\mathcal{M}_q,\mu_q)$ where $(\mathcal{M}_1,\mu_1)$ is a μ-extended tensor-mesh and $(\mathcal{M},\mu)=(\mathcal{M}_q,\mu_q)$. Moreover, $(\mathcal{M}_{j+1},\mu_{j+1})=(\mathcal{M}_j+\gamma_j,\mu_{j,\gamma_j})$ with γ_j a mesh-rectangle that splits $\mathcal{E}(\mathcal{M}_j)$ as in Definition 2.9, and μ_{j,γ_j} is as in Definition 2.11. We start with the complete collection $\mathcal{B}_1$ of tensor-product B-splines of degree $\boldsymbol{p}$ on $(\mathcal{M}_1,\mu_1)$. Suppose we have defined $\mathcal{B}_j$ for some $1\leqslant j<q$. We always assume that γ_j is such that there is a $B\in\mathcal{B}_j$ that does not have minimal support in $(\mathcal{M}_j+\gamma_j,\mu_{j,\gamma_j})$. We define $\mathcal{B}_{j+1}$ as follows.

1. As long as there is a $B\in\mathcal{B}_j$ that does not have minimal support in $(\mathcal{M}_{j+1},\mu_{j+1})$ we proceed as follows. Let γ be a (k,a)-mesh-rectangle that splits the support of B, where γ is a union of mesh-rectangles in $\mathcal{M}_{j+1}$. If $B(\boldsymbol{x})=B_1(x_1)\cdots B_d(x_d)$ for $\boldsymbol{x}=(x_1,\dots,x_d)\in\mathbb{R}^d$ then we insert a in the univariate B-spline B_k using (6) and get two univariate B-splines $B_{k,1}$ and $B_{k,2}$, and two tensor-product B-splines obtained from B by replacing B_k by $B_{k,1}$ and $B_{k,2}$, respectively.

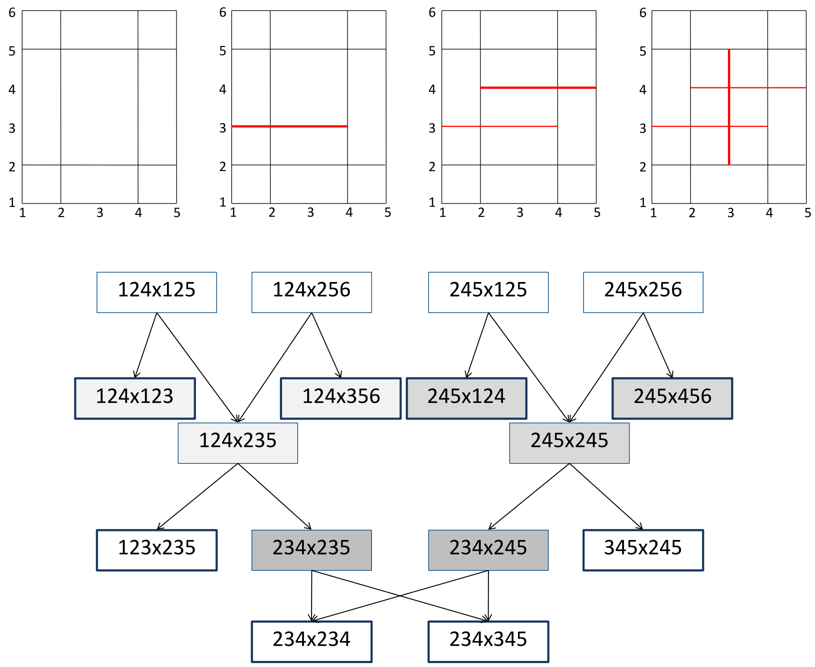

Fig. 9. Bilinear spline insertion and graph. Initial mesh (left), final mesh (right), corresponding graph (bottom). The B-splines on the final mesh are represented in the graph by nodes having no outgoing edges.

We update $\mathcal{B}_j$ by removing B and adding the two new tensor-product B-splines. We also remove duplicate B-splines if necessary.

2. When all $B \in \mathcal{B}_j$ have minimal support we set $\mathcal{B}_{j+1} = \mathcal{B}_j$.

Note that the process of going from $\mathcal{B}_j$ to $\mathcal{B}_{j+1}$ often involves a number of steps resulting in a sequence of LR B-spline collections $\mathcal{B}_{j,1}, \mathcal{B}_{j,2}, \ldots, \mathcal{B}_{j,r_j}$, where $\mathcal{B}_{j,1} = \mathcal{B}_j$ and $\mathcal{B}_{j,r_j} = \mathcal{B}_{j+1}$. We can combine all these collections into a global sequence of B-spline collections

$$(\tilde{\mathcal{B}}_1, \tilde{\mathcal{B}}_2, \ldots, \tilde{\mathcal{B}}_s) = (\mathcal{B}_{1,1}, \ldots, \mathcal{B}_{1,r_1}, \mathcal{B}_{2,1}, \ldots, \mathcal{B}_{2,r_2}, \ldots, \mathcal{B}_{q,1}, \ldots, \mathcal{B}_{q,r_q}). \tag{28}$$

Fig. 9 illustrates a bilinear example. The initial tensor-product mesh, with all knot multiplicities equal to one, is shown top left. First the horizontal line segment $[1,4] \times \{3\}$ is inserted (top second from left) splitting the two B-splines 124×125 and 124×256 into three B-splines depicted in light gray in the graph. Then the horizontal line segment $[2,5] \times \{4\}$ is inserted (top second from right) splitting the two B-splines 245×125 and 245×256 into three depicted in medium gray in the graph. Then the vertical line segment $\{3\} \times [2,5]$ is inserted (top right), splitting two B-splines 124×235 and 245×245 into four. However, two of these (depicted in dark gray in the graph) are split by the two first knot lines inserted, resulting in two B-splines at the bottom of the graph.

The collection $\mathcal{B}$ of LR B-splines only depends on the final mesh $\mathcal{M}$. The proof of the following theorem is found in Appendix A.

Theorem 3.4. *The collection $\mathcal{B}$ of LR B-splines in Section 3.2 does not depend on the order of insertion of the mesh-rectangles or the order of the subsequent single refinements.*

When given a μ-extended LR-mesh a practical way of constructing the LR B-splines is to start from the tensor product Bernstein basis based on the boundary of the LR-mesh, and successively refining according to the procedure of this subsection. Theorem 3.4 ensures that the final collection of B-splines is independent of the refinement sequence.

4. Spline spaces

In Section 3 the construction of the LR B-splines was addressed. In this section we will consider the structure and dimension of spline spaces over box-meshes.

4.1. Spline spaces over box-meshes

Let $\mathcal{E}$ be a box partition of $[\boldsymbol{a},\boldsymbol{b}]\in\mathbb{R}^d$ given as in Definition 2.2 and let $(\mathcal{M}(\mathcal{E}),\mu)$ be the corresponding μ-extended box-mesh. Let $\boldsymbol{p}=(p_1,\ldots,p_d)$ be a vector of nonnegative integers and set $\boldsymbol{x}^{\boldsymbol{i}}=x_1^{i_1}\cdots x_d^{i_d}$ for $\boldsymbol{i}=(i_1,\ldots,i_d)\geqslant\boldsymbol{0}$. We define polynomials of component degree at most p_k, $k=1,\ldots,d$ by

$$\Pi_{\boldsymbol{p}}^d:=\left\{f:\mathbb{R}^d\to\mathbb{R}\colon\ f(\boldsymbol{x})=\sum_{\boldsymbol{0}\leqslant\boldsymbol{i}\leqslant\boldsymbol{p}}c_{\boldsymbol{i}}\boldsymbol{x}^{\boldsymbol{i}},c_{\boldsymbol{i}}\in\mathbb{R}\text{ for all }\boldsymbol{i}\right\}.$$

Given a function $f:[\boldsymbol{a},\boldsymbol{b}]\to\mathbb{R}$, and let $\gamma\in\mathcal{F}_{d-1,k}(\mathcal{E})$ be any k-mesh-rectangle in $[\boldsymbol{a},\boldsymbol{b}]$ for some $1\leqslant k\leqslant d$. We say that $f\in C^r(\gamma)$ if the partial derivatives $\partial^j f(\boldsymbol{x})/\partial x_k^j$ exist and are continuous for $j=0,1,\ldots,r$ and all $\boldsymbol{x}\in\gamma$.

Definition 4.1. We define the piecewise polynomial space[5]

$$\mathbb{P}_{\boldsymbol{p}}(\mathcal{E}):=\left\{f:[\boldsymbol{a},\boldsymbol{b}]\to\mathbb{R}\colon\ f|_\beta\in\Pi_{\boldsymbol{p}}^d,\ \beta\in\tilde{\mathcal{E}}\right\},\tag{29}$$

where $\tilde{\mathcal{E}}$ is obtained from $\mathcal{E}$ by using half open intervals $[c_{i,k},e_{i,k})$ if $e_{i,k}<b_k$ and closed intervals otherwise. We define the spline space

$$\mathbb{S}_{\boldsymbol{p}}(\mathcal{M},\mu):=\left\{f\in\mathbb{P}_{\boldsymbol{p}}\big(\mathcal{E}(\mathcal{M})\big)\colon\ f\in C^{p_k-\mu(\gamma)}(\gamma),\ \forall\gamma\in\mathcal{F}_{d-1,k}^o(\mathcal{M}),\ k=1,\ldots,d\right\}.\tag{30}$$

We also set

$$\mathbb{S}_{\boldsymbol{p}}(\mathcal{M}):=\left\{f\in\mathbb{P}_{\boldsymbol{p}}\big(\mathcal{E}(\mathcal{M})\big)\colon\ f\in C^{p_k-1}(\gamma),\ \forall\gamma\in\mathcal{F}_{d-1,k}^o(\mathcal{M}),\ k=1,\ldots,d\right\}.\tag{31}$$

The use of $\tilde{\mathcal{E}}$ instead of $\mathcal{E}$ ensures that each $\boldsymbol{x}\in[\boldsymbol{a},\boldsymbol{b}]$ belongs to exactly one of the sub-boxes.

4.2. Dimension of spline spaces over box-meshes

In Mourrain (2010) the dimensionality of spline spaces over planar T-subdivisions when the continuity across mesh-rectangles is fixed in both parameter directions, is addressed. This idea inspired a generalization in Pettersen (2013). In that paper the dimension of a spline over a μ-extended box-mesh in $\mathbb{R}^d$ is addressed, and the following dimension formula presented

$$\begin{aligned}\dim\mathbb{S}_{\boldsymbol{p}}(\mathcal{M},\mu)&=\sum_{\ell=0}^{d-1}(-1)^{d-\ell}\left(\sum_{\beta\in\mathcal{F}_\ell(\mathcal{M})}\prod_{k=1}^{d}\big(p_k-\mu_k(\beta)+1\big)\right)\\&\quad+f_d\prod_{k=1}^{d}(p_k+1)-\sum_{\ell=0}^{d-1}(-1)^{d-\ell}\dim H_\ell,\end{aligned}\tag{32}$$

where $f_d:=\#(\mathcal{F}_d(\mathcal{M}))$ is the number of elements in $\mathcal{E}(\mathcal{M})$ and

$$\mu_k(\beta)=\max\big(\{0\}\cup\left\{\mu(\gamma)\colon\ \beta\subset\gamma\in\mathcal{F}_{d-1,k}(\mathcal{M})\right\}\big).\tag{33}$$

- The first sum is only dependent on the topology of the box-mesh by relating to the degree and mesh-rectangle continuity $(p_k-\mu_k(\beta)+1)$.
- The second sum contains homology terms, H_ℓ, $\ell=0,\ldots,d-1$, that can be regarded as correction factors in the case when the topological counting over all boxes in $\mathcal{F}$ is not sufficient to determine the dimensionality of the spline space. See Pettersen (2013) and examples below for more details.

Example 4.2. Consider the univariate ($d=1$) case and a knot vector

$$t_1\leqslant t_2\leqslant\cdots\leqslant t_n=\eta_1^{[\mu_1]}<\cdots<\eta_m^{[\mu_m]},\tag{34}$$

where $n:=\sum_{i=1}^m\mu_i$, $m\geqslant 2$, and $1\leqslant\mu_i\leqslant p+1$, $i=1,\ldots,m$. Using (32) we obtain

[5] We can also use variable degrees. Suppose for each $\beta\in\mathcal{E}$ there is a vector $\boldsymbol{p}_\beta\in\mathbb{R}^d$ with nonnegative integer components. $\mathbb{P}_{\boldsymbol{p}}(\mathcal{E}):=\{f:[\boldsymbol{a},\boldsymbol{b}]\to\mathbb{R}\colon\ f|_\beta\in\Pi_{\boldsymbol{p}_\beta}^d,\ \beta\in\tilde{\mathcal{E}}\}$.

$$\begin{aligned}\dim \mathbb{S}_{\boldsymbol{p}}(\mathcal{M},\mu) &= -\sum_{\beta\in\mathcal{F}_0(\mathcal{M})}\big(p-\mu(\beta)+1\big)+(m-1)(p+1)+\dim H_0\\ &= -\sum_{i=1}^{m}(p-\mu_i+1)+(m-1)(p+1)+\dim H_0\\ &= n-p-1+\dim H_0=(n-p-1)_+ =: \max(0,n-p-1).\end{aligned}$$

The last equality follows from Pettersen (2013) where it is shown that $\dim H_0=(p+1-n)_+$. Thus $\dim H_0=0$ in the normal case where $n\geqslant p+1$.

For $d=2$ Eq. (32) becomes

$$\begin{aligned}\dim \mathbb{S}_{\boldsymbol{p}}(\mathcal{M},\mu) = &\sum_{\beta\in\mathcal{F}_0(\mathcal{M})}\big(p_1-\mu_1(\beta)+1\big)\big(p_2-\mu_2(\beta)+1\big)\\ &-\sum_{\beta\in\mathcal{F}_{1,1}(\mathcal{M})}\big(p_1-\mu_1(\beta)+1\big)(p_2+1)\\ &-\sum_{\beta\in\mathcal{F}_{1,2}(\mathcal{M})}(p_1+1)\big(p_2-\mu_2(\beta)+1\big)\\ &+f_2(p_1+1)(p_2+1)-\dim H_0+\dim H_1.\end{aligned} \tag{35}$$

Example 4.3. Consider the two-dimensional tensor-product case.

$$t_{k,1}\leqslant\cdots\leqslant t_{k,n_k}=\eta_{k,1}^{[\mu_{k,1}]}<\cdots<\eta_{k,m_k}^{[\mu_{k,m_k}]}, \tag{36}$$

where $m_k\geqslant 2$ and $1\leqslant\mu_{k,i}\leqslant p_k+1$, $i=1,\ldots,m_k$, $k=1,2$. Eq. (35) becomes

$$\begin{aligned}\dim \mathbb{S}_{\boldsymbol{p}}(\mathcal{M},\mu) &= \sum_{i=1}^{m_1}\sum_{j=1}^{m_2}(p_1-\mu_{1,i}+1)(p_2-\mu_{2,j}+1)\\ &\quad-\sum_{i=1}^{m_1}\sum_{j=1}^{m_2-1}(p_1-\mu_{1,i}+1)(p_2+1)\\ &\quad-\sum_{i=1}^{m_1-1}\sum_{j=1}^{m_2}(p_1+1)(p_2-\mu_{2,j}+1)\\ &\quad+(m_1-1)(m_2-1)(p_1+1)(p_2+1)-\dim H_0+\dim H_1\\ &=\left(\sum_{i=1}^{m_1-1}(p_1+1)-\sum_{i=1}^{m_1}(p_1-\mu_{1,i}+1)\right)\\ &\quad\cdot\left(\sum_{j=1}^{m_2-1}(p_2+1)-\sum_{j=1}^{m_2}(p_2-\mu_{2,j}+1)\right)-\dim H_0+\dim H_1\\ &=(n_1-p_1-1)(n_2-p_2-1)-\dim H_0+\dim H_1\\ &=(n_1-p_1-1)_+(n_2-p_2-1)_+,\end{aligned}$$

since it follows from Pettersen (2013) that

$$\begin{aligned}\dim H_0&=(p_1+1-n_1)_+(p_2+1-n_2)_+,\\ \dim H_1&=(n_1-p_1-1)_+(p_2+1-n_2)_+ + (p_1+1-n_1)_+(n_2-p_2+1)_+.\end{aligned}$$

Example 4.4. Consider the two-dimensional box-mesh, where the multiplicity of boundary edges is equal to the degree $+1$ in both parameter directions giving $\mu(\gamma^v)=p_1+1$ for vertical boundary edges γ^v, and $\mu(\gamma^h)=p_2+1$ for horizontal boundary edges γ^h. Across all interior vertical edges we require the continuity to be C^{r_1}, $0\leqslant r_1<p_1$ implying multiplicity of $\mu(\gamma^v)=p_1-r_1$ for internal vertical edges γ^v. Across all horizontal interior edges we require the continuity to be C^{r_2}, $0\leqslant r_2<p_2$ implying multiplicity of $\mu(\gamma^h)=p_2-r_2$ for internal horizontal edges γ^h. With this in mind (35) reduces to

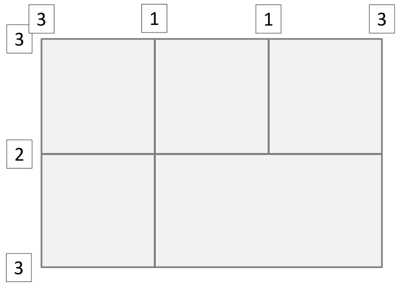

Fig. 10. A bi-quadratic case where the continuity across internal vertical edges is C^1, e.g., $r_1 = 1$, and the continuity across internal horizontal edges is C^0, e.g., $r_2 = 0$. (Remember continuity is degree minus multiplicity.) We find $\dim(\mathbb{S}_{\boldsymbol{p}}(\mathcal{M}, \mu)) = 3 \times 3F_2 - 3 \times 1F_1^h - 2 \times 3F_1^v + 2 \times 1F_0 = 22$ based on the counting: $F_2 = 5$, $F_1^h = 3$, $F_1^v = 3$, and $F_0 = 2$.

$$\begin{aligned}\dim \mathbb{S}_{\boldsymbol{p}}(\mathcal{M}, \mu) = {} & (p_1+1)(p_2+1)F_2 - (p_1+1)(r_2+1)F_1^h \\ & - (r_1+1)(p_2+1)F_1^v + (r_1+1)(r_2+1)F_0 \\ & - \dim H_0 + \dim H_1,\end{aligned} \tag{37}$$

where

- F_2 is the number of rectangles,
- F_1^h and F_1^v are the numbers of horizontal and vertical interior edges,
- F_0 is the number of interior vertices.

In Pettersen (2013) it is shown that $\dim H_0 = 0$ in this case, and $\dim H_1 = 0$ for the LR-mesh constructed in Section 3.2. The formula (37) corresponds to Mourrain (2010), where the homology terms are expressed using a different homology. For an example see Fig. 10.

5. Dimension increase and spanning property

It is important to establish the dimension increase when a mesh-rectangle is inserted, and situations where the LR B-splines span the full spline space defined by the μ-extended LR-mesh.

In the following definition we introduce a concept that formalizes the relation between the μ-extended LR-mesh $(\mathcal{M}, \mu)$ and its corresponding collection of LR B-splines $\mathcal{B}$.

Definition 5.1 *(Hand-in-hand LR-refinement).* Suppose $(\mathcal{M}, \mu, \boldsymbol{p})$ is a μ-extended LR-mesh in $\mathbb{R}^d$ with $\boldsymbol{p} \geqslant \mathbf{0}$ a given degree. Let $\mathcal{B}$ be the corresponding collection of LR B-splines of degree $\mathbf{p}$. Let γ be a constant split mesh-rectangle as in Definition 2.11, and $\mathcal{B}'$ the corresponding collection of LR B-splines of degree $\mathbf{p}$ on $(\mathcal{M}+\gamma, \mu_\gamma, \boldsymbol{p})$. We say that $(\mathcal{M}+\gamma, \mu_\gamma, \boldsymbol{p})$ goes **hand-in-hand** with $(\mathcal{M}, \mu, \boldsymbol{p})$ if $\operatorname{span}(B)_{B\in\mathcal{B}} = \mathbb{S}_{\boldsymbol{p}}(\mathcal{M}, \mu)$ and $\operatorname{span}(B)_{B\in\mathcal{B}'} = \mathbb{S}_{\boldsymbol{p}}(\mathcal{M}+\gamma, \mu_\gamma)$.

The following theorem gives a sufficient condition so that the collection of LR B-splines spans the spline space in the special case when the refinement leads to a dimension increase by one.

Theorem 5.2. *Let $(\mathcal{M}_1, \mu_1), (\mathcal{M}_2, \mu_2), \ldots, (\mathcal{M}_q, \mu_q) = (\mathcal{M}, \mu)$ be a sequence of μ-extended LR-meshes with corresponding collections of LR B-splines $\mathcal{B}_1, \ldots, \mathcal{B}_q$ of degree $\boldsymbol{p} \geqslant \mathbf{0}$ as in Section 3.2. If $\dim \mathbb{S}_{\boldsymbol{p}}(\mathcal{M}_{j+1}, \mu_{j+1}) = \dim \mathbb{S}_{\boldsymbol{p}}(\mathcal{M}_j, \mu_j) + 1$, $j = 1, \ldots, q-1$ then*

$$\mathbb{S}_{\boldsymbol{p}}(\mathcal{M}_j, \mu_j) = \operatorname{span}(B)_{B\in\mathcal{B}_j}, \quad j = 1, \ldots, q.$$

In other words, each step in the refinement process goes hand-in-hand.

Proof. As $\mathcal{B}_1$ is the tensor-product B-spline basis over $(\mathcal{M}_1, \mu_1)$ it follows that $\mathbb{S}_{\boldsymbol{p}}(\mathcal{M}_1, \mu_1) = \operatorname{span}(B)_{B\in\mathcal{B}_1}$.

Now assume that $\mathbb{S}_{\boldsymbol{p}}(\mathcal{M}_{j-1}, \mu_{j-1}) = \operatorname{span}(B)_{B\in\mathcal{B}_{j-1}}$, for some $j > 1$. From the assumption we know that $\dim(\mathbb{S}_{\boldsymbol{p}}(\mathcal{M}_j, \mu_j)) = \dim(\mathbb{S}_{\boldsymbol{p}}(\mathcal{M}_{j-1}, \mu_{j-1})) + 1$. The collection of B-splines $\mathcal{B}_j$ has to contain some minimal support B-splines not in $\mathcal{B}_{j-1}$. These B-splines are linearly independent of the B-splines in $\mathcal{B}_{j-1}$ as they contain part of a mesh-rectangle counting multiplicity, not in $(\mathcal{M}_{j-1}, \mu_{j-1})$. Consequently $\dim(\operatorname{span}(B)_{B\in\mathcal{B}_j}) \geqslant \dim(\operatorname{span}(B)_{B\in\mathcal{B}_{j-1}}) + 1$. However, these new B-splines belong to $\mathbb{S}_{\boldsymbol{p}}(\mathcal{M}_j, \mu_j)$. Consequently $\mathbb{S}_{\boldsymbol{p}}(\mathcal{M}_j, \mu_j) = \operatorname{span}(B)_{B\in\mathcal{B}_j}$. $\square$

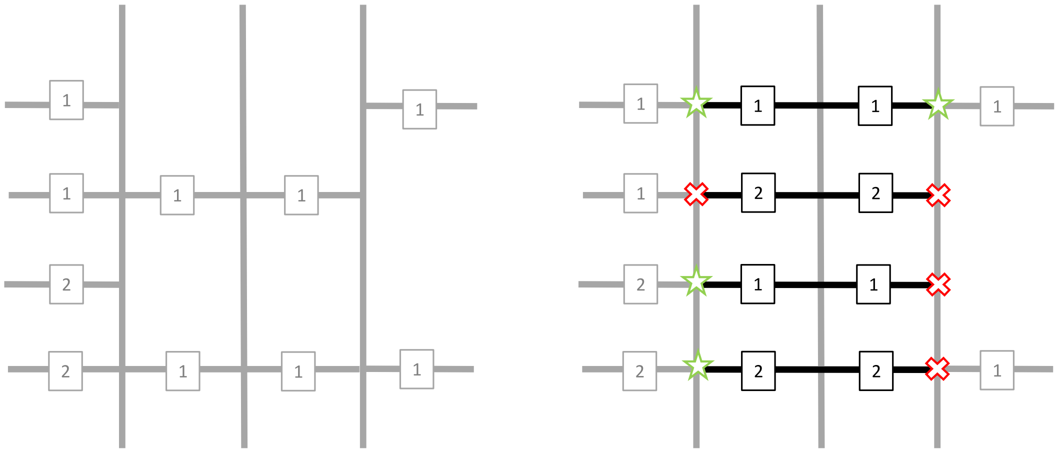

Fig. 11. This illustration shows attachment of 4 inserted horizontal segments. Only mesh-rectangles in the same hyperplane as the inserted mesh-rectangle have to be considered and vertical multiplicities are irrelevant for this example. Going from top to bottom the first segment has multiplicity 1 and is attached at both ends. The next segment has multiplicity 2 while there is no horizontal neighboring segment to the right and the one to the left has multiplicity one. This segment is not attached at either end. The third and fourth segments are both attached at the left end, but not at the right.

5.1. Refinements in 2-dimensional meshes

We now look at how we can describe the spline space dimension change for refinements on a 2-dimensional mesh, and how this is used to test the hand-in-hand property of LR B-splines.

In this subsection we consider the following situation. Suppose $(\mathcal{M}, \mu, \boldsymbol{p})$ is a general μ-extended LR-mesh in $\mathbb{R}^2$ and $\boldsymbol{p} = (p_1, p_2) \geqslant \boldsymbol{0}$ a given bidegree. Let the 2-mesh-rectangle $\gamma = [b, e] \times \{a\}$ be a constant split of $(\mathcal{M}, \mu)$. Let (b_j, a), $j = 1, 2, \ldots, n$ with $b = b_1 < b_2 < \cdots < b_n = e$ be the points defined by the intersection of γ and all vertical mesh-rectangles in $\mathcal{M}$.

Definition 5.3. Given $(\mathcal{M}, \mu, \boldsymbol{p})$ and a constant split $\gamma = [b, e] \times \{a\}$ of $(\mathcal{M}, \mu)$ of multiplicity $m := \mu(\gamma)$ as above, and let $\boldsymbol{q}$ be one of the endpoints (b, a) or (e, a) of γ. Let $\mu_2(\boldsymbol{q})$ be the horizontal multiplicity as given by (24) with respect to $(\mathcal{M}, \mu)$. We say that γ is **attached to** $(\mathcal{M}, \mu)$ at $\boldsymbol{q}$ if $\mu_2(\boldsymbol{q}) \geqslant m$.

Examples of different attachments are shown in Fig. 11 and considered in Example 5.7.

Definition 5.4. Define $\tilde{\mu}_1, \ldots, \tilde{\mu}_n$ to be the vertical multiplicities $\tilde{\mu}_i = \mu_1(b_i, a)$ except that $\tilde{\mu}_1 = p_1 + 1$ if γ is attached to $(\mathcal{M}, \mu)$ at $\boldsymbol{q}_1 := (b, a)$ and $\tilde{\mu}_n = p_1 + 1$ if γ is attached to $(\mathcal{M}, \mu)$ at $\boldsymbol{q}_2 := (e, a)$. If γ is a 1-mesh-rectangle, the multiplicities $\tilde{\mu}_i$ and attachment properties are defined in the same way by swapping the parameter directions.

The following result describes the dimension change during refinements on a mesh in $\mathbb{R}^2$, based on the dimensional formula in (35). Figs. 12 and 13 illustrate the different configurations.

Theorem 5.5. *Suppose $(\mathcal{M}, \mu, \boldsymbol{p})$ is a μ-extended LR-mesh in $\mathbb{R}^2$ and $\boldsymbol{p} = (p_1, p_2) \geqslant \boldsymbol{0}$ a given bidegree. Let the mesh-rectangle γ be a constant split of $(\mathcal{M}, \mu)$, and let $\tilde{\mu}_i$ be as in Definition 5.4. Then*

$$\dim \mathbb{S}_{\boldsymbol{p}}(\mathcal{M} + \gamma, \mu_\gamma) = \dim \mathbb{S}_{\boldsymbol{p}}(\mathcal{M}, \mu) + \sum_{i=1}^{n} \tilde{\mu}_i - p - 1 + \Delta h_1 - \Delta h_0, \tag{38}$$

where Δh_i is the change in the dimension of the homology term H_i in (35), and where $p = p_1$ if γ is a 2-mesh-rectangle and $p = p_2$ if γ is a 1-mesh-rectangle.

Proof. We assume $\gamma = [b, e] \times \{a\}$ is a horizontal 2-mesh-rectangle of multiplicity $m := \mu_\gamma(\beta)$ after insertion. The multiplicity before insertion is $\mu(\beta) := m - 1$. The case for 1-mesh-rectangles is similar. Let $b = b_1 < b_2 < \cdots < b_n = e$ be the knots such that (b_i, a), $i = 1, \ldots, n$ are the points in $\mathcal{F}_0(\mathcal{M} + \gamma)$ that lie on γ. We look at how the combinatorial part of the dimension formula changes from $(\mathcal{M}, \mu)$ to $(\mathcal{M} + \gamma, \mu_\gamma)$ by considering the contribution to the dimension changes into two parts:

Part 1. *2-boxes and 2-mesh-rectangles*: For given $i = 1, \ldots, n - 1$, we are looking for changes on 2-boxes on the form $[b_i, b_{i+1}] \times J$ for a nontrivial interval $J := [a_1, a_2]$ containing a, and for the 2-mesh-rectangle $\beta = [b_i, b_{i+1}] \times \{a\}$. If $m = 1$, β

did not exist in $\mathcal{M}$. We then replace the 2-box $[b_i, b_{i+1}] \times [a_1, a_2]$ by the 2-boxes $[b_i, b_{i+1}] \times [a_1, a]$ and $[b_i, b_{i+1}] \times [a, a_2]$, $a_1 < a < a_2$, this gives a combinatorial change in (35) of $+(p_1 + 1)(p_2 + 1)$. Also, the introduction of β gives a formula change of $-(p_1 + 1)(p_2 - \mu_\gamma(\beta) + 1) = -(p_1 + 1)p_2$. Altogether the change is $(p_1 + 1)(p_2 + 1) - (p_1 + 1)p_2 = p_1 + 1$. And if $m > 1$, nothing is changed to the topological structure of $\mathcal{M}$, but we get a change in the dimension formula for β which is

$$\begin{aligned} &-\big[-(p_1+1)\big(p_2-\mu(\beta)+1\big)\big]+\big[-(p_1+1)\big(p_2-\mu_\gamma(\beta)+1\big)\big] \\ &\quad =(p_1+1)\big[\big(p_2-(m-1)+1\big)-(p_2-m+1)\big]=p_1+1 \end{aligned}$$

just as for $m = 1$. So for any m, the total change for all i is $(n - 1)(p_1 + 1)$.

Part 2. 1-*mesh-rectangles and points*: For given $i = 1, \dots, n$, we are looking for changes on 1-mesh-rectangles on the form $\{b_i\} \times J$ for a nontrivial interval $J := [a_1, a_2]$ containing a, and for the point $\beta = (b_i, a)$. If $m = 1$ and (for $i = 1$ or n), γ is not attached to $(\mathcal{M}, \mu)$ at β, we replace (like for case 1) the 1-mesh-rectangle $\{b_i\} \times [a_1, a_2]$ with the mesh-rectangles $\{b_i\} \times [a_1, a]$ and $\{b_i\} \times [a, a_2]$. This means going from 1 to 2 contributions of $-(p_1 - \tilde{\mu}_i + 1)(p_2 + 1)$. At the same time β comes in with the contribution $(p_1 - \tilde{\mu}_i + 1)(p_2 - m + 1)$. The total change is

$$(p_1-\tilde{\mu}_i+1)(p_2-m+1)-(p_1-\tilde{\mu}_i+1)(p_2+1)=\tilde{\mu}_i-p_1-1$$

because $m = 1$. If $m > 1$ and (for $i = 1$ or n), γ is not attached to $(\mathcal{M}, \mu)$ at β, the dimension formula changes at β by

$$-(p_1-\tilde{\mu}_i+1)\big(p_2-\mu_1(\beta)+1\big)+(p_1-\tilde{\mu}_i+1)\big(p_2-(\mu_\gamma)_1(\beta)+1\big)=\tilde{\mu}_i-p_1-1,$$

just as for $m = 1$. Finally, if γ is attached to $(\mathcal{M}, \mu)$ at β, nothing changes because $\mu_1(\beta) = (\mu_\gamma)_1(\beta) \geqslant m$. But then $\tilde{\mu}_i = p_1 + 1$, so regardless of the value of m and whether γ is attached to $(\mathcal{M}, \mu)$ at β or not, the change is $\tilde{\mu}_i - p_1 - 1$. Summing this up for all i gives a change of

$$\sum_{i=1}^{n}\tilde{\mu}_i-n(p_1+1).$$

Combining parts 1 and 2 the total change is

$$(n-1)(p_1+1)+\sum_{i=1}^{n}\tilde{\mu}_i-n(p_1+1)=\sum_{i=1}^{n}\tilde{\mu}_i-p_1-1,$$

giving the change in the dimension formula. The result about the homology terms follows from Pettersen (2013). □

The homology terms in Theorem 5.5 are zero in certain cases.

1. $H_0 = 0$ in (35) as long as $\mathbb{S}_{\boldsymbol{p}}(\mathcal{M}, \mu)$ is nontrivial (contains other spline functions than the zero function),
2. $H_1 = 0$ for an ordinary tensor-mesh.
3. $\Delta h_1 \leqslant 0$ if $\sum_i \tilde{\mu}_i \geqslant p_k + 1$. In particular, if $H_1 = 0$ in the dimension formula for $\dim \mathbb{S}_{\boldsymbol{p}}(\mathcal{M}, \mu)$ then $H_1 = 0$ for $\dim \mathbb{S}_{\boldsymbol{p}}(\mathcal{M} + \gamma, \mu_\gamma)$. This follows since we assumed in Section 3.2 that γ splits at least one B-spline so that $\sum_i \tilde{\mu}_i \geqslant p_k + 2$.

We next consider the special case of LR-meshes with interior mesh-rectangles of multiplicity one.

Corollary 5.6. *Suppose $d = 2$ and that $\mathcal{M}_1$ is a $(p_1 + 1, p_2 + 1)$ regular tensor-mesh, i.e., the boundary faces have multiplicity $p_k + 1$, $k = 1, 2$. Assume $\mu(\gamma) = 1$ for all interior mesh-rectangles γ in $\mathcal{M}_j$, $j = 1, \dots, q$. Then $\dim \mathbb{S}_{\boldsymbol{p}}(\mathcal{M}_{j+1}) = \dim \mathbb{S}_{\boldsymbol{p}}(\mathcal{M}_j) + 1$, $j = 1, \dots, q - 1$ in the following three cases.*

[A] *For $k = 1, 2$ each new k-mesh-rectangle intersects exactly $p_{3-k} + 2$ interior orthogonal mesh-rectangles and ends in interior T-vertices at both ends.*
[B] *An existing mesh-rectangle is extended with one segment that ends in an interior T-vertex.*
[C] *The inserted mesh-rectangle starts at the boundary and intersects exactly one interior orthogonal mesh-rectangle, and ends in an interior T-vertex.*

Proof. For these kinds of insertions it follows from the discussion after Theorem 5.5 that the homology terms are zero. Consider (38). In all three cases it is easy to see that $\sum_{i=1}^{n} \tilde{\mu}_i - p - 1 = 1$, where $p = p_1$ for a horizontal segment and $p = p_2$ for a vertical one. □

The three cases are illustrated in Fig. 12.

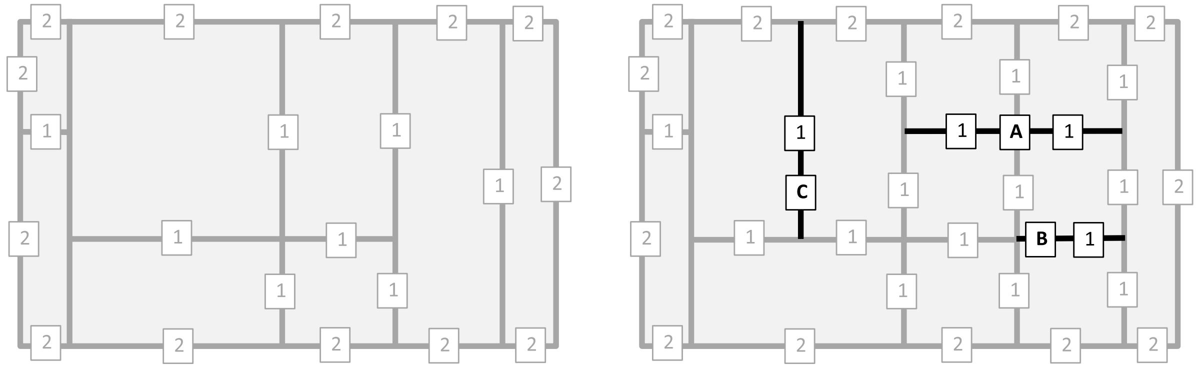

Fig. 12. To the left a bi-linear μ-extended LR-mesh illustrating the 3 cases in Corollary 5.6. The multiplicity is 2 along the boundary, and 1 for interior mesh-rectangles. Mesh-rectangle A has two segments and ends in a T-vertex at both ends; Mesh-rectangle B extends an interior mesh-rectangle by one segment and ends in a T-vertex; Mesh-rectangle C starts from the boundary, and has one segment. Note that extending C to touch the lower boundary would increase the dimension of the spline space by two, and is thus not covered in Corollary 5.6.

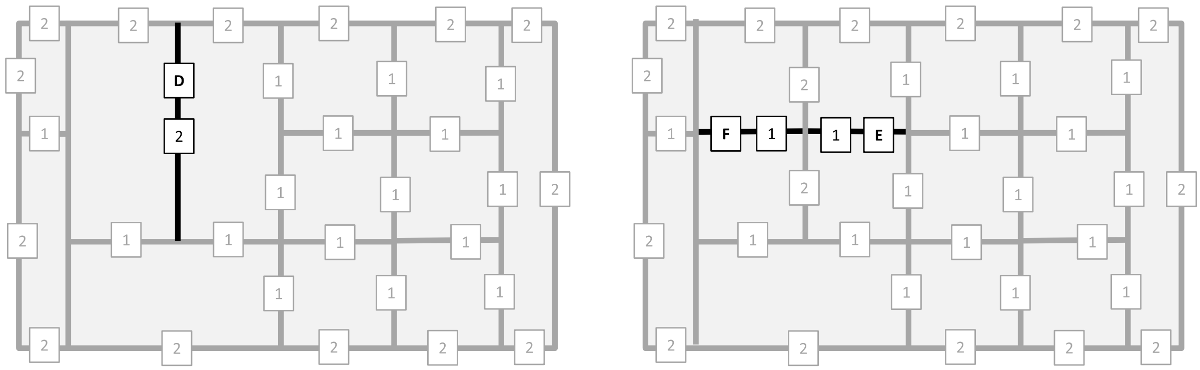

Fig. 13. The illustration shows refinements related to mesh-rectangles of multiplicity higher than 1, and to the filling of gaps between already existing mesh-rectangles. To the left the result of the refinement in Fig. 12 with mesh-rectangle D inserted on top of mesh-rectangle C, thus increasing the multiplicity from 1 to 2. To the right we first insert the mesh-rectangle E (mesh-rectangle F has not been inserted yet) that ends in a T-vertex with multiplicity 2. This increases the dimension of the spline space by 2. Then we fill a gap by mesh-rectangle F, that further increases the dimension of the spline space by 2.

The following example addresses the 2-variate case when the refinement goes hand-in-hand and has a dimension increase by 1.

Example 5.7. In Theorem 5.5 assume that $\operatorname{span}(B)_{B\in\mathcal{B}} = \mathbb{S}_{\boldsymbol{p}}(\mathcal{M},\mu)$, and that the homology terms H_0 and H_1 are zero, and that $\sum_i \tilde{\mu}_i = p+2$. In this case the homology terms remain zero, and we have $\dim \mathbb{S}_{\boldsymbol{p}}(\mathcal{M}+\gamma,\mu_\gamma) = \dim \mathbb{S}_{\boldsymbol{p}}(\mathcal{M},\mu)+1$. By Theorem 5.2 $(\mathcal{M},\mu)$ goes hand-in-hand with $\mathbb{S}_{\boldsymbol{p}}(\mathcal{M}+\gamma,\mu_\gamma)$.

Now consider in more detail the possible attachment relations for γ.

- If γ is attached at no end, we have a mesh-rectangle spanning exactly the width of the domain of one or more B-splines. The sum of the multiplicities of the orthogonal mesh-rectangles intersected equals $p+2$.
- If γ is attached at one end, the other end has to have multiplicity 1, and the number of vertices on γ has to be 2, i.e., there are no interior vertices on γ.
- If $p \geqslant 1$ it is not possible that γ is attached at both ends as each attachment imposes multiplicity of $p+1$, contradicting the assumption $\sum_i \tilde{\mu}_i = p+2$.

Recall that n is the number of points defined by the intersection of γ and all orthogonal mesh-rectangles in $\mathcal{M}$. In the case when $n>2$ and $\sum_i \tilde{\mu}_i - p_1 - 1 > 1$ we can often, but not always, split the refinement into a sequence of refinements each giving a dimension increase by one, and then use the results of Example 5.7.

When $n=2$ we cannot split the refinement into a sequence of smaller refinements and obtain a dimension increase greater than one in the following cases, see Fig. 13 (right).

- **Attachment at both ends**. If $n=2$ and $\tilde{\mu}_1 = \tilde{\mu}_2 = p+1$ we get a dimension increase of $\sum_i \tilde{\mu}_i - p - 1 = p+1$. This is the case in gap filling.

- **Attachment at one end**. With $n = 2$ we have for example $\tilde{\mu}_1 = p + 1$ and $\tilde{\mu}_2 > 1$, giving a dimension increase $\sum_i \tilde{\mu}_i - p - 1 = \tilde{\mu}_2 > 1$.

How to determine if the hand-in-hand condition is satisfied in the cases above is addressed in Section 5.2.

For completeness we also address the case when $\sum_i \tilde{\mu}_i - p - 1 \leqslant 0$ in Theorem 5.5, i.e., situations where we do not split any LR B-spline.

Example 5.8. Suppose $\sum_i \tilde{\mu}_i - p - 1 \leqslant 0$, assume in Theorem 5.5 that $\operatorname{span}(B)_{B\in\mathcal{B}} = \mathbb{S}_{\boldsymbol{p}}(\mathcal{M}, \mu)$, and that the homology terms H_0 and H_1 are zero. In this case γ cannot be attached at any end since then the first or last $\tilde{\mu}_i$ is equal to $p + 1$, implying that the other end has multiplicity 0, i.e., that γ has length zero.

- If $\sum_i \tilde{\mu}_i - p - 1 < 0$, there is a risk that the homology term increases. Such a refinement will never split any LR B-spline, so it is not relevant case for LR B-splines.
- If $\sum_i \tilde{\mu}_i - p - 1 = 0$, we know that the homology terms remain zero. But the spline space does not change since now $\dim \mathbb{S}_{\boldsymbol{p}}(\mathcal{M} + \gamma, \mu_\gamma) = \dim \mathbb{S}_{\boldsymbol{p}}(\mathcal{M}, \mu)$ as demonstrated in Theorem 5.5. We do not split any LR B-spline, but this case can be useful as an intermediate state in some refinements.

5.2. More complex refinements

The study of when two μ-extended meshes go hand-in-hand is simplified by considering the restriction B_γ of a B-spline B to a mesh-rectangle γ. More precisely we have the following definition.

Definition 5.9. Let $B : \mathbb{R}^d \to \mathbb{R}$ be a tensor-product B-spline given by

$$B(x_1, \ldots, x_d) = B[\boldsymbol{y}_1, \ldots, \boldsymbol{y}_d](x_1, \ldots, x_d) = \prod_{i=1}^{d} B[\boldsymbol{y}_i](x_i), \tag{39}$$

and $\gamma = J_1 \times \cdots \times J_d \subseteq \mathbb{R}^d$ a (k, a)-mesh-rectangle. Define $\tilde{\gamma} = J_1 \times \cdots \times J_{k-1} \times J_{k+1} \times \cdots \times J_d \subseteq \mathbb{R}^{d-1}$.

We define the $(d-1)$-variate B-spline $B_\gamma : \mathbb{R}^{d-1} \to \mathbb{R}$ by

$$B_\gamma(\boldsymbol{x}) = \begin{cases} \prod_{\substack{i=0 \\ i\neq k}}^{d} B[\boldsymbol{y}_i](x_i) & \text{for } \boldsymbol{x} \in \tilde{\gamma}, \\ 0 & \text{for } \boldsymbol{x} \notin \tilde{\gamma} \end{cases}$$

for every $\boldsymbol{x} = (x_1, \ldots, x_{k-1}, x_{k+1}, \ldots, x_d) \in \mathbb{R}^{d-1}$.

A lower bound for the increase in dimension when a mesh-rectangle is inserted can be determined from a collection of B_γ's. We even have equality when the two corresponding meshes go hand-in-hand.

Theorem 5.10. *Suppose $(\mathcal{M}, \mu, \boldsymbol{p})$ is a μ-extended LR-mesh in $\mathbb{R}^d$ with $\boldsymbol{p} \geqslant \boldsymbol{0}$ a given degree. Let γ be a constant split (k, a)-mesh-rectangle in $\mathbb{R}^d$ of multiplicity $\mu(\gamma)$ (cf. Definition 2.11) and let $\mathcal{B}$ and $\mathcal{B}'$ be the corresponding collection of LR B-splines of degree* $\mathbf{p}$ *on $(\mathcal{M}, \mu, \boldsymbol{p})$ and $(\mathcal{M} + \gamma, \mu_\gamma, \boldsymbol{p})$, respectively. Let $\mathcal{B}'(\gamma)$ be the collection of all LR B-splines $B \in \mathcal{B}'$ such that $\operatorname{supp}(B)^o \cap \gamma \neq \emptyset$, and such that the knot a occurs with multiplicity $\mu(\gamma)$ in the knot vector $\boldsymbol{y}_k$ when B is written on the form (39). If $\operatorname{span}(B)_{B\in\mathcal{B}} = \mathbb{S}_{\boldsymbol{p}}(\mathcal{M}, \mu)$, then*

$$\dim \operatorname{span}(B_\gamma)_{B\in\mathcal{B}'(\gamma)} \leqslant \dim \mathbb{S}_{\boldsymbol{p}}(\mathcal{M} + \gamma, \mu_\gamma) - \dim \mathbb{S}_{\boldsymbol{p}}(\mathcal{M}, \mu),$$

where B_γ is defined in Definition 5.9. Equality holds if and only if $(\mathcal{M} + \gamma, \mu_\gamma, \boldsymbol{p})$ goes hand-in-hand with $(\mathcal{M}, \mu, \boldsymbol{p})$.

Proof. Define $m := \mu(\gamma) - 1$ and let $F : \mathbb{R}^d \to \mathbb{R}$ be a spline function in $\mathbb{S}_{\boldsymbol{p}}(\mathcal{M} + \gamma, \mu_\gamma)$. For sufficiently small $\epsilon > 0$ the functions $F^+ = F|_{\mathbb{R}^{k-1}\times(a,a+\epsilon)\times\mathbb{R}^{d-k}}$ and $F^- = F|_{\mathbb{R}^{k-1}\times(a-\epsilon,a)\times\mathbb{R}^{d-k}}$ are polynomial in x_k, i.e.,

$$F^+ = \sum_{i=0}^{p_k} f_i^+ (x_k - a)^i,$$

$$F^- = \sum_{i=0}^{p_k} f_i^- (x_k - a)^i$$

for spline functions f_i^+, f_i^- in the variables $(x_1, \ldots, x_{k-1}, x_{k+1}, \ldots, x_d)$. The expressions for F^+ and F^- can be used to extend them to functions on $\mathbb{R}^d$. Let $\gamma^+ = J_1 \times \cdots \times J_{k-1} \times \mathbb{R} \times J_{k+1} \times \cdots \times J_d$. We define the jump function $J(F)$ on $\mathbb{R}^d$ to be $F^+ - F^-$ on γ^+ and 0 outside γ^+. Because $F \in \mathbb{S}_{\boldsymbol{p}}(\mathcal{M} + \gamma, \mu_\gamma)$, it is $C^{(p_k-m-1)}$ over γ, therefore we have

$$J(F) = \sum_{i=p_k-m}^{p_k} J(F)_i (x_k - a)^i$$

for some spline functions $J(F)_i$ on $\mathbb{R}^{d-1}$. If we let $\mathbb{S}^{d-1}$ be the set of all spline functions in $d-1$ variables, we now have a linear map $\phi : \mathbb{S}_{\boldsymbol{p}}(\mathcal{M}+\gamma, \mu_\gamma) \to \mathbb{S}^{d-1}$ defined by $\phi(F) = J(F)_{p_k-m}$.

The only difference in the smoothness constraints between $\mathbb{S}_{\boldsymbol{p}}(\mathcal{M}, \mu)$ and $\mathbb{S}_{\boldsymbol{p}}(\mathcal{M}+\gamma, \mu_\gamma)$ is that functions in $\mathbb{S}_{\boldsymbol{p}}(\mathcal{M}+\gamma, \mu_\gamma)$ are $C^{(p_k-m-1)}$ while functions in $\mathbb{S}_{\boldsymbol{p}}(\mathcal{M}, \mu)$ are $C^{(p_k-m)}$ over γ. Therefore the kernel of ϕ is $\mathbb{S}_{\boldsymbol{p}}(\mathcal{M}, \mu) = \operatorname{span}(B)_{B\in\mathcal{B}}$ and we have inclusions

$$\ker\phi = \mathbb{S}_{\boldsymbol{p}}(\mathcal{M}, \mu) = \operatorname{span}(B)_{B\in\mathcal{B}} \subseteq \operatorname{span}(B)_{B\in\mathcal{B}'} \subseteq \mathbb{S}_{\boldsymbol{p}}(\mathcal{M}+\gamma, \mu_\gamma).$$

For any linear map $\psi : V \to W$ between vector spaces, we have $\dim\ker\psi + \dim\psi(V) = \dim V$, therefore

$$\dim\mathbb{S}_{\boldsymbol{p}}(\mathcal{M}, \mu) + \dim\operatorname{span}\big(\phi(B)\big)_{B\in\mathcal{B}'} = \dim\operatorname{span}(B)_{B\in\mathcal{B}'} \leqslant \dim\mathbb{S}_{\boldsymbol{p}}(\mathcal{M}+\gamma, \mu_\gamma).$$

Therefore the result of the theorem follows if we can show $\operatorname{span}(J(B)_{p_k-m})_{B\in\mathcal{B}'} = \operatorname{span}(B_\gamma)_{B\in\mathcal{B}'(\gamma)}$.

For a B-spline function on the form (39), a jump across a k-mesh-rectangle γ, can be expressed as a jump in the k-th parameter direction, giving

$$J(B) = J'\big(B[\boldsymbol{y}_k]\big) \prod_{\substack{i=1 \\ i\neq k}}^{d} B[\boldsymbol{y}_i]$$

on γ^+ and 0 outside γ^+, where $J'(f)$ is the jump function of a univariate spline f over x_k in $x_k = a$ given as the difference between the polynomial expressions of f on the left-hand and right-hand sides of a. If we write

$$J'\big(B[\boldsymbol{y}_k]\big) = \sum_{i=0}^{d} J'\big(B[\boldsymbol{y}_k]\big)_i (x_k - a)^i$$

it is well known that if M is the multiplicity of a in $\boldsymbol{y}_k$, the numbers $J'(B[\boldsymbol{y}_k])_i$ are zero for $i \leqslant p_k - M$ and nonzero for $i = p_k - M + 1$ (if $M > 0$). We then have $J(B)_{p_k-m} = J'(B[\boldsymbol{y}_k])_{p_k-m} B_\gamma$. Suppose $B \in \mathcal{B}'$. If $\operatorname{supp}(B) \cap \gamma = \emptyset$, the function B_γ is zero, and if a occurs at most m times in $\boldsymbol{y}_k$, then $J'(B[\boldsymbol{y}_k])_{p_k-m} = 0$. Therefore $J(B)_{p_k-m}$ is nonzero if and only if $B \in \mathcal{B}'(\gamma)$. Therefore $\operatorname{span}(J(B)_{p_k-m})_{B\in\mathcal{B}'} = \operatorname{span}(B_\gamma)_{B\in\mathcal{B}'(\gamma)}$, completing the proof. □

Theorem 5.10 reduces the problem of establishing when the refinement goes hand-in-hand to finding the dimension of the $(d-1)$-dimensional B-spline space $\dim\operatorname{span}(\mathcal{B}'(\gamma))$ and see if it is equal to $\dim\mathbb{S}_{\boldsymbol{p}}(\mathcal{M}+\gamma, \mu_\gamma) - \dim\mathbb{S}_{\boldsymbol{p}}(\mathcal{M}, \mu)$. In the examples following we will address the 2-variate case, in which $\mathcal{B}'(\gamma)$ spans a univariate spline space restricted to γ. We will for all examples assume that γ is minimal in the sense that the refinement cannot be split into a sequence using shorter mesh-rectangles.

Example 5.11 *(Attachment at no end).* There are two cases:

- $\sum_i \tilde{\mu}_i - p - 1 = 1$. In this case the dimension increase is just 1, and the hand-in-hand holds if $\mathcal{B}'(\gamma)$ contains at least one B-spline.
- $\sum_i \tilde{\mu}_i - p - 1 > 1$. In order to verify the hand-in-hand property we have to find $\dim\operatorname{span}(B_\gamma)_{B\in\mathcal{B}'(\gamma)}$, the dimension of a univariate spline space, and see that this is the same as $\sum_i \tilde{\mu}_i - p - 1$.

Example 5.12 *(Attachment at one end).* As the refinement cannot be split into subrefinements it follows that $n = 2$, and $\operatorname{span}((B_\gamma)_{B\in\mathcal{B}'(\gamma)})$ is a polynomial space for which we have to find the dimension. However, as the B-splines in question all stop at the end of γ that is not attached, it suffices to find a subcollection $(B_i)_{i=1}^{\sum_i \tilde{\mu}_i - p - 1}$ of $(B_\gamma)_{B\in\mathcal{B}'(\gamma)}$ such that B_i has a knot of multiplicity i at this end.

Example 5.13 *(Attachment at both ends).* Also in this case we need to find $\dim\operatorname{span}((B_\gamma)_{B\in\mathcal{B}'(\gamma)})$. By inserting knots in $(B_\gamma)_{B\in\mathcal{B}'(\gamma)}$ such that the knot multiplicity at both ends of γ is $p+1$ we can express $(B_\gamma)_{B\in\mathcal{B}'(\gamma)}$ in terms of the Bernstein basis of degree p via the Oslo Algorithm. The rank of the knot insertion matrix determines $\dim\operatorname{span}(B_\gamma)_{B\in\mathcal{B}'(\gamma)}$.

The next examples look at the C^2 and C^1 bi-cubic cases when all boundary mesh-rectangles have multiplicity 4. We assume that the refinements are minimal.

Example 5.14. In the C^2 bi-cubic case the interior mesh-rectangles have multiplicity 1. There are six cases, three with a dimension increase by 1, three with a dimension increase by 4.

- The cases of dimension increase 1 go hand-in-hand are addressed in Corollary 5.6 cases [A], [B] and [C]:
  - Attachment at no end and not touching the boundary at any end.
  - Attachment at one end, the other end not touching the boundary.
  - Attachment at no end, touching the boundary at one end.
- The cases of dimension increase 4 have $\tilde{\mu}_i = 4$ at both ends,
  - Attachment at no end and touching the boundary at both ends.
  - Attachment at one end, the other end touching the boundary.
  - Attachment at both ends.

  Theorem 5.10 shows that the dimension increase can be determined by looking at the univariate B-splines restricted to γ, and check if they span a univariate spline space of dimension 4 on γ. Since there are no interior knots this can be done by conversion to the cubic Bernstein basis on γ and check the rank of the corresponding knot insertion matrix.

Example 5.15. In the C^1 bi-cubic case all interior mesh-rectangles have multiplicity 2. We have six cases, three with a dimension increase by 2, three with a dimension increase by 4.

- The three cases of dimension increase 2 are:
  - Attachment at no end and not touching the boundary at any end. In this case there are three points on γ each with $\tilde{\mu}_i = 2$.
  - Attachment at one end with the other end not touching the boundary. In this case there are two points on γ, the attachment point has $\tilde{\mu}_i = 4$, while the other point has $\tilde{\mu}_i = 2$.
  - Attachment at no end and touching the boundary at one end. In this case there are two points on γ, the boundary point has $\tilde{\mu}_i = 4$, while the other point has $\tilde{\mu}_i = 2$.

  According to Theorem 5.5 we have a dimension increase of $\sum_i \tilde{\mu}_i - p - 1 = 6 - 3 - 1 = 2$. However, as the B-splines in question all stop at the end of γ that is not attached or touching the boundary, it suffices to find two B-splines in $(B_\gamma)_{B \in \mathcal{B}'(\gamma)}$ such that one has a knot of multiplicity 1 at this end, and the other has multiplicity 2 at this end.
- The three cases of dimension increase 4 are the same as those addressed in Example 5.14 for the C^2 case.

6. Linear independence

For the use of LR B-splines in isogeometric analysis it is essential to ensure that they are linearly independent. For T-splines linear independence does not hold in general (Buffa et al., 2010; Li and Chen, 2011), and a class of analysis suitable T-splines (Scott et al., 2011) has been introduced by requiring that the knotline segments (mesh-rectangles) not spanning the full width of the domain are not allowed to intersect. This is a strong restriction on the grid. However, the restriction has the advantage that it can be checked before a refinement is performed.

Rather than imposing such severe restrictions an alternative is to check if each refinement results in a collection of linearly independent LR B-splines. For linear independence of the LR B-splines it is sufficient that the refinements go hand-in-hand, see Definition 5.1, and that the increase in the number of B-splines going from $(\mathcal{M}_j, \boldsymbol{\mu}_j, \boldsymbol{p})$ to $(\mathcal{M}_{j+1}, \boldsymbol{u}_{j+1}, \boldsymbol{p})$ equals the increase in dimension of the corresponding spline spaces for all j. Example 6.4 below, illustrated in Fig. 16, shows that this is not always the case.

However, there are other criteria based on the spanning property, that if fulfilled, are sufficient for ensuring that a collection of LR B-splines over a μ-extended LR-mesh is linearly independent. The LR B-spline refinement process creates a nested sequence of refinement spaces, starting with a tensor product B-spline spaces spanning the full polynomial space over each element. Consequently at each refinement step there will be at least $(p_1+1)(p_2+1)\ldots(p_d+1)$ B-splines covering each element, and the full polynomial space will be spanned on each element.

Definition 6.1. We say that an element is **overloaded** if there are more B-splines covering the element than is necessary for spanning the corresponding polynomial space. We call a B-spline **overloaded** if all the elements in its support are overloaded.

A consequence of this definition is that local and global linear independence of the collection of LR B-splines is ensured if there are no overloaded elements.

Lemma 6.2. *In a collection of LR B-splines only overloaded B-splines can occur in a linear dependency relation.*

Proof. Assume that we have a linear dependency relation that includes at least one B-spline that is not overloaded, then at least one of the elements of this B-spline is not overloaded. If we remove this B-spline the element will be covered by less than $(p_1 + 1)(p_2 + 1)\ldots(p_d + 1)$ B-splines contradicting the fact that the full polynomial space is spanned on each element. □

A consequence of this lemma is that if there are no overloaded B-splines in the μ-extended LR-mesh then the B-splines are locally and globally linearly independent.

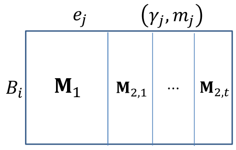

Fig. 14. The incidence matrix $\boldsymbol{M}$.

Given a $\boldsymbol{\mu}$-extended LR-mesh $(\mathcal{M}, \boldsymbol{\mu})$ and a set $\mathcal{B} := \{B_1, \ldots, B_r\}$ of tensor product B-splines of degree $\boldsymbol{p}$ with support in $(\mathcal{M}, \boldsymbol{\mu})$. From $\mathcal{B}$ we define an incidence matrix $\boldsymbol{M}$, where each row corresponds to a B-spline in $\mathcal{B}$ (See Fig. 14).

We have $\boldsymbol{M} = [\boldsymbol{M}_1, \boldsymbol{M}_2]$, where the columns of $\boldsymbol{M}_1$ represent the elements $e_1, \ldots, e_s$ in the mesh $\mathcal{M}$, while the columns of $\boldsymbol{M}_2$ represent all mesh-rectangles $\beta_1, \ldots, \beta_t$ in $\mathcal{M}$ repeated according to their multiplicity. More specifically $\boldsymbol{M}_2 = [\boldsymbol{M}_{2,1}, \ldots, \boldsymbol{M}_{2,t}]$, where each $\boldsymbol{M}_{2,k}$ has $\mu(\beta_k)$ columns. To start these matrices are defined as follows.

$$M_1(i,j) := \begin{cases} 1, & \text{if } e_j \subset \operatorname{supp} B_i, \\ 0, & \text{otherwise,} \end{cases} \qquad M_{2,k}(i,j) := \begin{cases} 1, & j = 1, \ldots, m_{i,k}, \\ 0, & \text{otherwise,} \end{cases}$$

where $m_{i,j}$ is the multiplicity of β_j in B_i. Defining $M_{2,k}$ in this way, we can distinguish between B-splines with different continuity across β_k.

We can find B-splines in $\mathcal{B}$ that cannot be part of a linear dependency relation in two ways:

- Suppose column j in $\boldsymbol{M}_1$ contains a single 1 in say, row i. Then there is only one B-spline B_i with support on e_j. This B-spline cannot be part of a linear dependency relation in $\mathcal{B}$.
- Suppose column j in $\boldsymbol{M}_{2,k}$ contains a single 1 in say, row i. Then B_i is the only B-spline in $\mathcal{B}$ with a knotline of multiplicity at least j on β_k, and this B-spline cannot be part of a linear dependency relation in $\mathcal{B}$.

In both cases we can cancel B_i from $\mathcal{B}$ by setting row i in $\boldsymbol{M}$ to zero. This leads to the following algorithm.

Algorithm 6.3 *(Pealing algorithm).* As long as there is a j such that $M_{i,j} = 1$ for some i, and $M_{i',j} = 0$ for all $i' \neq i$, set $M_{i,j'} = 0$ for all j'. Repeat until no such j is found.

The algorithm terminates with an $\boldsymbol{M}$ that is zero or nonzero. If $\boldsymbol{M} = \mathbf{0}$, then the B-splines in $\mathcal{B}$ are linearly independent, while if $\boldsymbol{M} \neq \mathbf{0}$ then a possible linear dependency relation in $\mathcal{B}$ can only involve those B_i such that row i in the final matrix $\boldsymbol{M}$ is nonzero. Let $\mathcal{B}'$ be the collection of these B-splines.

When $\mathcal{B}'$ is not empty we have to check if the B-splines in $\mathcal{B}'$ are linearly independent or not. This can be done by knot insertion to create a local tensor product basis, and check if the rank of the refinement matrix corresponds to the number of B-splines. However, in many cases we expect more direct approaches to be sufficient. Note that

- if an element is covered by exactly two B-splines from $\mathcal{B}'$ then the two B-splines can take part in the linear dependency relation only if they differ by a scale factor over the element,
- if only two B-splines from $\mathcal{B}'$ have a discontinuity in the same derivative across a mesh-rectangle the two B-spline can only take part in the linear dependency relation if the discontinuity is the same apart from a nonzero scaling factor.

The algorithm is applied to a collection of overloaded B-splines in Fig. 15.

Example 6.4 *(Linear dependence).* Suppose $p_1 = p_2 = 2$, and all mesh-rectangles have multiplicity 1. In the μ-extended LR-mesh to the left in Fig. 16 we insert the vertical segment $4 \times [1,2]$. The two tensor-product B-splines $(1,2,3,6) \times (1,2,4,5)$ and $(3,6,8,9) \times (1,2,3,4)$ are refined. We remove these two and get 4 new B-splines $(1,2,3,4) \times (1,2,4,5)$, $(2,3,4,6) \times (1,2,4,5)$, $(3,4,6,8) \times (1,2,3,4)$ and $(4,6,8,9) \times (1,2,3,4)$. Thus the number of B-splines increases by two, while the dimension of $\mathbb{S}_{2,2}(\mathcal{M}, \mu)$ only increases by one. So there is one B-spline too much in $\mathcal{B}$.

Different strategies can be employed to address the issue of a refinement resulting in too many B-splines and thus producing a collection of B-splines that is not a basis for $\mathbb{S}_{\boldsymbol{p}}(\mathcal{M}, \mu)$.

- *Discard refinement.* We discard the problematic refinement, for example when the pealing algorithm terminates with $\boldsymbol{M} \neq \mathbf{0}$, and choose an alternative refinement in the vicinity that does not have this problem. The approach is simple, and seems not to restrict the flexibility of the refinement much. Testing indicates that the situation of too many B-splines occurs very seldom. E.g., in the bi-cubic case typically in 0.01% of the refinements tested.
- *Perform extra refinement.* Another possibility is to include the problematic mesh-rectangle in the process and continue inserting mesh-rectangles until, hopefully the number of B-splines matches the dimension of the spline space.

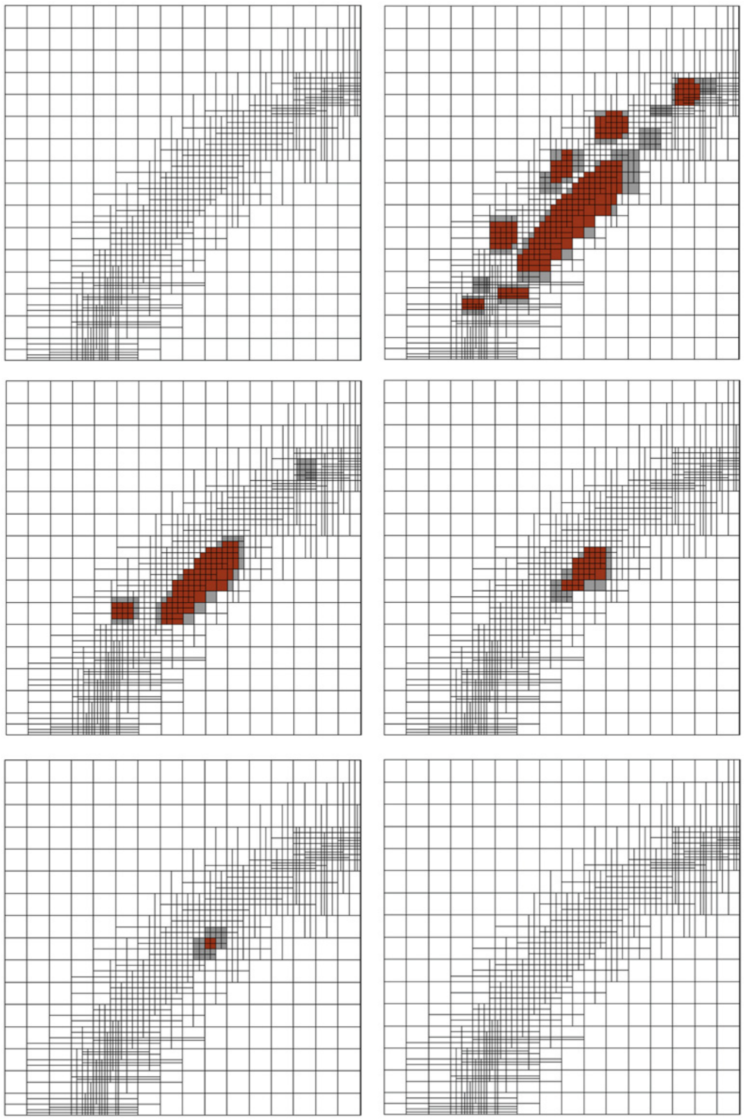

Fig. 15. The illustration at the top to the left shows an LR-mesh. In the top right illustration the elements with only one overloaded B-spline are colored light gray, while elements with two or more overloaded B-splines are colored dark gray (red in the web version). In the following illustrations overloaded B-splines are removed according to the pealing algorithm, ending up with a grid without overloaded B-splines, thus showing that the collection of LR B-splines is linearly independent.

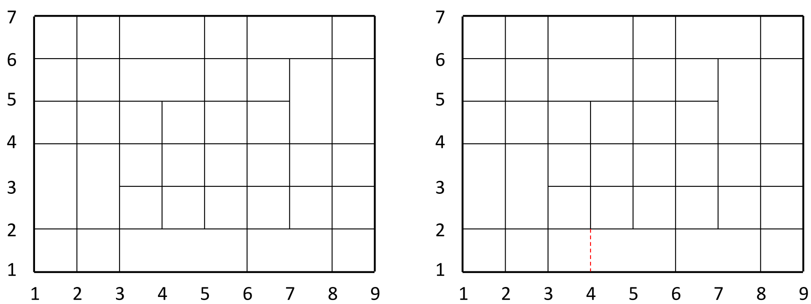

Fig. 16. Linear dependence of bi-quadratic LR B-splines. In this LR-mesh all mesh-rectangles have multiplicity 1.

- *Eliminate a B-spline.* The dependencies of the basis functions in Fig. 16 can be expressed as follows

$$\begin{aligned}720B[2368;1246] = {} & 108B[5678;2346]+135B[2356;2456]\\ & +108B[3567;3456]+268B[3456;2345]\\ & +324B[4567;2345]+360B[2346;1245]\\ & +384B[3468;1234]. \end{aligned} \tag{40}$$

  Thus the basis function $B[2368;1246]$ can be replaced and positive weights maintained. Testing in the bi-cubic case shows that such positive substitution can be done in around 80% of the cases. If the elimination does not allow such positive isolation of the B-spline eliminated, the result can potentially be that the elimination will produce a basis where some basis functions have a negative weight when scaled to form a partition of unity.

7. Partition of unity

The nonnegative partition of unity property of tensor-product B-splines gives the convex hull property, and is essential for interpreting the B-spline coefficients as control points. After performing local refinement the LR B-splines will generally not sum to one. Consequently adjustments of the new collection of LR B-splines that reinstate the partition of unity property is necessary. It is also important to preserve nonnegativity. Let $\mathcal{B}$ be a collection of LR B-splines, and assume that the span of these B-splines contains constants. To turn $\mathcal{B}$ into a partition of unity collection we see two alternatives:

- **Rational scaling**. We make a scaled partition of unity collection $\mathcal{B}^R$ of $\mathcal{B}$ by

$$\mathcal{B}^R=\left(\frac{B}{\sum_{B'\in\mathcal{B}}B'}\right)_{B\in\mathcal{B}}. \tag{41}$$

- **Scaling by weights**. We make a weighted partition of unity $\mathcal{B}^S := (B^S := \gamma_B B)_{B\in\mathcal{B}}$ by introducing weights γ_B such that

$$\sum_{B\in\mathcal{B}}\gamma_B B\equiv 1. \tag{42}$$

In general T-splines employ rational scaling to ensure partition of unity.

We will in the following use scaling by weights since rational basis functions are harder to differentiate. Recall, see (28), that the process of going from $\mathcal{B}_1$ to the final collection $\mathcal{B}_q$ of LR B-splines can be described by a sequence $(\tilde{\mathcal{B}}_k)_{k=1}^s$. Going from $\tilde{\mathcal{B}}_k$ to $\tilde{\mathcal{B}}_{k+1}$ involves picking a B-spline $B_0\in\tilde{\mathcal{B}}_k$ that can be split and use univariate knot insertion as described in (6) to obtain two new B-splines,

$$B_0=\alpha_1B_1+\alpha_2B_2. \tag{43}$$

Then

$$\tilde{\mathcal{B}}_{k+1}=\big(\tilde{\mathcal{B}}_k\setminus\{B_0\}\big)\cup\{B_1,B_2\}.$$

Note that B_1 and/or B_2 could already belong to $\tilde{\mathcal{B}}_k$. The proof of the following lemma is found in Appendix B.

Lemma 7.1. *Given k with $1\leqslant k\leqslant s-1$, suppose $\sum_{B\in\tilde{\mathcal{B}}_k}\gamma_{k,B}B=1$ for some positive $\gamma_{k,B}\in\mathbb{R}$. Then $\sum_{B\in\tilde{\mathcal{B}}_{k+1}}\gamma_{k+1,B}B=1$, where for $B\in\tilde{\mathcal{B}}_{k+1}$ the $\gamma_{k+1,B}$ are all positive and more precisely $\gamma_{k+1,B}=\gamma_{k,B}$, if $B\in\tilde{\mathcal{B}}_k\setminus\{B_0,B_1,B_2\}$, and*

$$\gamma_{k+1,B_l}=\begin{cases}\gamma_{k,B_0}\alpha_l, & \text{if } B_l\notin\tilde{\mathcal{B}}_k,\\ \gamma_{k,B_l}+\gamma_{k,B_0}\alpha_l, & \text{if } B_l\in\tilde{\mathcal{B}}_k,\end{cases}\qquad l=1,2, \tag{44}$$

where $B_0,B_1,B_2,\alpha_1,\alpha_2$ are given by (43). If $f=\sum_{B\in\tilde{\mathcal{B}}_k}c_{k,B}\gamma_{k,B}B$ for some $c_{k,B}\in\mathbb{R}$ then $f=\sum_{B\in\tilde{\mathcal{B}}_{k+1}}c_{k+1,B}\gamma_{k+1,B}B$, where $c_{k+1,B}=c_{k,B}$, if $B\in\tilde{\mathcal{B}}_{k+1}\setminus\{B_0,B_1,B_2\}$ and

$$c_{k+1,B_l}=\begin{cases}c_{k,B_0}, & \text{if } B_l\notin\tilde{\mathcal{B}}_k,\\ (c_{k,B_l}\gamma_{k,B_l}+c_{k,B_0}\gamma_{k,B_0}\alpha_l)/\gamma_{k+1,B_l}, & \text{if } B_l\in\tilde{\mathcal{B}}_k,\end{cases}\qquad l=1,2. \tag{45}$$

The stability of univariate B-splines is described by condition numbers. In the univariate case a constant K can be found such that $\frac{1}{K}\|\mathbf{c}\|_\infty\leqslant\|\sum_j c_jB_j\|_\infty\leqslant\|\mathbf{c}\|_\infty$. Moreover, K only depends on the degree of the B-splines. Since univariate B-splines form a nonnegative partition of unity the upper bound follows trivially. We now show that the same upper bound holds for the scaled LR B-splines. Finding a lower bound for LR B-splines is an open question.

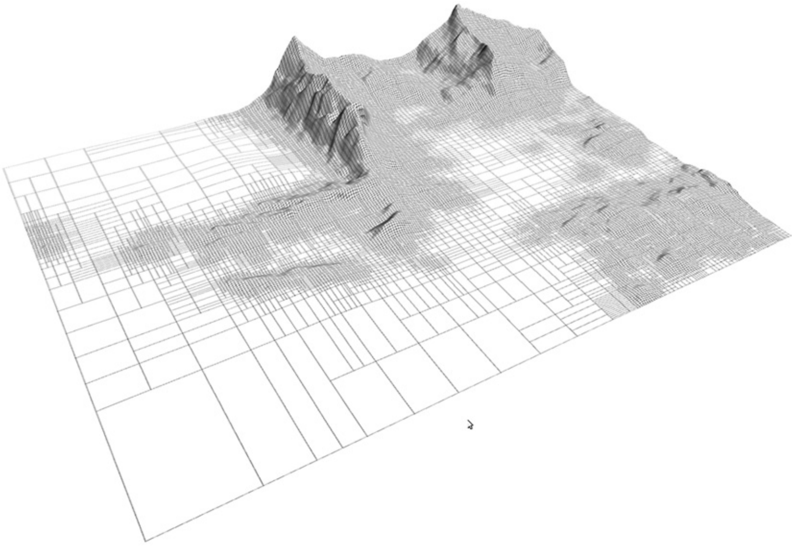

Fig. 17. An example of a C^2 bi-cubic approximation of a large set of terrain data from the area of Svolvaer Airport in the North of Norway. The LR-mesh is projected as a texture on to the surface showing the piecewise structure of the approximation. The data used is courtesy of Avinor, Norway.

Theorem 7.2. *For the final collection $\mathcal{B} = \mathcal{B}_q$ of LR B-splines (cf. Section 3.2), there exist positive constants $\gamma_B \in \mathbb{R}$ giving a nonnegative partition of unity*

$$\sum_{B\in\mathcal{B}} N_B = 1 \quad \text{where } N_B := \gamma_B B.$$

If $f = \sum_{B\in\mathcal{B}} c_B N_B : [\boldsymbol{a}, \boldsymbol{b}] \to \mathbb{R}$ for some $c_B \in \mathbb{R}$ we have the lower and upper bound

$$\min_{B\in\mathcal{B}} c_B \leqslant f(\boldsymbol{x}) \leqslant \max_{B\in\mathcal{B}} c_B, \quad \boldsymbol{x} \in [\boldsymbol{a}, \boldsymbol{b}].$$

In particular,

$$\|f\|_\infty \leqslant \left\|(c_B)_{B\in\mathcal{B}}\right\|_\infty.$$

If $\boldsymbol{c}_B \in \mathbb{R}^s$ for all $B \in \mathcal{B}$ and some $s \geqslant 2$ then the convex hull property holds, i.e., f lies in the convex hull of $(\boldsymbol{c}_B)_{B\in\mathcal{B}}$.

Proof. This follows from Lemma 7.1 by noting that $\gamma_B = \gamma_{s,B}$ and $c_B = c_{s,B}$. $\square$

8. Comparing LR B-splines and T-splines

The main difference between LR B-splines and T-splines is how the B-splines are defined:

- For LR B-splines the refinement is specified in the parameter domain by a mesh-rectangle refining at least one B-spline, thus the refinement is directly related to the sequence of nested spline spaces generated by the LR B-spline refinement process. LR B-splines assign mesh-rectangle multiplicity and are compatible with the approach of univariate B-splines.
- T-splines are defined from anchors in (the index space version of) the T-mesh, see Bazilevs et al. (2010), where a T-mesh is defined as a rectangular tiling of a region in $\mathbb{R}^2$. For odd degree each vertex in the T-mesh is an anchor that is used together with the T-mesh to define a corresponding (rationally scaled) tensor product B-spline. For even degree the anchors are situated at the center of every rectangle in the T-mesh. The T-mesh is refined by inserting new anchors. In some cases nestedness of the sequence of corresponding spline spaces spanned by the B-splines is lost.
- By projecting the LR-grid onto the 3D surface, see Fig. 17, we create a control mesh on the surface, thus allowing specification of the mesh-rectangle on the surface. The mesh-rectangle can be specified by its end points. Alternatively a T-splines like approach can be followed by anchoring the mid-point of the mesh-rectangle in the LR-mesh.

9. Conclusions and remaining challenges

This paper is a first step in establishing a theoretical foundation for the theory of LR-splines and a practical framework for the implementation of LR B-splines.[6] The emphasis has been on generality. We have introduced the hand-in-hand strategy to ensure that the LR B-splines span the spline space defined by the LR-mesh. For the 2-variate case we have discussed how this can be used for ensuring linear independence of the LR B-splines. In addition to linear independence in higher dimensions and conditioning of the basis, a number of open questions still remains to be solved:

- The hand-in-hand strategy is based on the homology terms being zero. This is well understood in the 2-variate case, see Mourrain (2010), Pettersen (2013). In general understanding the homology terms is more complex, especially since in higher dimensions elements can touch each other in many ways that possibly might give nonzero homology terms.
- We have in the 2-variate case defined 3 attachment configurations that help understand and structure the use of the hand-in-hand concept. The number of attachment configurations is significantly higher in the 3-variate case, as mesh rectangles can touch and intersect in many ways.
- In univariate spline theory Marsdens identity (Schumaker, 2007) gives closed expressions for the reproduction of polynomials. Coefficients for writing polynomials in terms of LR B-splines can be updated during the refinement process, but it would be nice to have closed expressions.
- In univariate spline theory the Schoenberg–Whitney theorem states exactly where to select interpolation points in order to guaranty a unique interpolant. Uniqueness of interpolation for LR B-splines has not been touched in this paper.
- We have not addressed where to refine, consequently there are many open questions related to the numerical stability of different refinement strategies.

Appendix A. LR B-splines are well defined

In this appendix we prove Theorem 3.4. It is based on two lemmas.

The first step is to look at sequences of univariate splines. For this we need a definition.

Definition A.1. Given two knot vectors $\boldsymbol{t} = (t_1, \dots, t_m)$ and $\boldsymbol{\tau} = (\tau_1, \dots, \tau_n)$. We say that $\boldsymbol{t}$ **includes** $\boldsymbol{\tau}$ if $t_1 \leqslant \tau_1$ and $t_m \geqslant \tau_n$, and in the case $t_1 = \tau_1$, the multiplicity (number of occurrences) of t_1 in $\boldsymbol{t}$ is at least the same as the multiplicity of τ_1 in $\boldsymbol{\tau}$, and in the case $t_m = \tau_n$, the multiplicity of t_m in $\boldsymbol{t}$ is at least the same as the multiplicity of τ_n in $\boldsymbol{\tau}$.

Lemma A.2. *Given a degree p, sequences $B_{\boldsymbol{t}_1}, \dots, B_{\boldsymbol{t}_n}$ of univariate p-degree B-splines, $\tau_2, \dots, \tau_n$ of real numbers and $s_2, \dots, s_n \in \{1, 2\}$ such that for every $i = 2, \dots, n$, $\tau_i \in (t_{i-1,1}, t_{i-1,p+2})$, and $\boldsymbol{t}_i = R(\boldsymbol{t}_{i-1}, \tau_i, s_i)$. Also given $\nu \in (t_{1,1}, t_{1,p+2})$. Then there is a sequence $B_{\boldsymbol{t}'_1}, \dots, B_{\boldsymbol{t}'_n}$ of univariate p-degree B-splines and a $\sigma \in \{1, 2\}$ such that*

- $\boldsymbol{t}'_1 = R(\boldsymbol{t}_1, \nu, \sigma)$.
- *$\boldsymbol{t}_i$ includes $\boldsymbol{t}'_i$ for $i = 1, \dots, n$.*
- *For every $i = 2, \dots, n$, either $\boldsymbol{t}'_i = \boldsymbol{t}'_{i-1}$ or $\boldsymbol{t}'_i = R(\boldsymbol{t}'_{i-1}, \tau_i, s'_i)$ for some $s'_i = 1$ or 2.*
- *For the smallest i such that $\tau_i = \nu$ (if any), we have $\boldsymbol{t}'_i = \boldsymbol{t}'_{i-1}$.*

Proof. We use induction on n. For $n = 1$, we can chose σ to be either 1 or 2, both will work. Next we assume $n > 1$ and that the lemma holds for B-spline sequences of length $n - 1$. We can also restrict to the case $s_2 = 2$ as $s_2 = 1$ is identical by symmetry. We have four cases:

Case 1, both $t_{1,2} < \nu$, $t_{1,2} < \tau_2$ and $\nu \neq \tau_2$. We derive $\boldsymbol{t}_2$ from $\boldsymbol{t}_1$ by removing $t_{1,1}$ and inserting τ_2. From the assumptions we have $t_{2,1} = t_{1,2} < \nu < t_{1,p+2} = t_{2,p+2}$. Therefore we can use the lemma on the sequences $B_{\boldsymbol{t}_2}, \dots, B_{\boldsymbol{t}_n}$, $\tau_3, \dots, \tau_n$ and $s_3, \dots, s_n$, which by the induction hypothesis gives us the desired sequence $B_{\boldsymbol{t}'_2}, \dots, B_{\boldsymbol{t}'_n}$ where $\boldsymbol{t}'_2 = R(\boldsymbol{t}_2, \nu, \sigma')$ for some $\sigma' \in \{1, 2\}$. We put $\sigma = 2$ and $s'_2 = \sigma'$. We derive $\boldsymbol{t}'_2$ from $\boldsymbol{t}_2$ by removing $(t_{1,p+2}, t_{1,2})_{\sigma'}$ (i.e. $t_{1,p+2}$ if $\sigma' = 1$ and $t_{1,2}$ if $\sigma' = 2$) and inserting ν, and so $\boldsymbol{t}'_2$ is derived from $\boldsymbol{t}_1$ by removing $t_{1,1}$ and $(t_{1,p+2}, t_{1,2})_{\sigma'}$ and inserting ν and τ_2. If we define $\boldsymbol{t}'_1 = R(\boldsymbol{t}_1, \nu, \sigma)$, we derive $\boldsymbol{t}'_1$ from $\boldsymbol{t}_1$ by removing $t_{1,1}$ and inserting ν. But then $\boldsymbol{t}'_2 = R(\boldsymbol{t}'_1, \tau_2, s'_2)$ and we are done.

Case 2, $\nu = \tau_2$. Put $\sigma = 2$, and $\boldsymbol{t}'_1 := R(\boldsymbol{t}_1, \nu, \sigma) = R(\boldsymbol{t}_1, \tau_2, s'_2) = \boldsymbol{t}_2$. We can then put $\boldsymbol{t}'_i = \boldsymbol{t}_i$ for $i = 2, \dots, n$. Because $\boldsymbol{t}'_2 = \boldsymbol{t}'_1$, we are done.

Case 3, both $\nu \leqslant t_{1,2}$ and $\nu < \tau_2$. Put $\sigma = s'_2 = 2$, $\boldsymbol{t}'_1 := R(\boldsymbol{t}_1, \nu, \sigma)$ and $\boldsymbol{t}'_2 := R(\boldsymbol{t}'_1, \nu, s'_2)$. Then $\boldsymbol{t}'_2$ is derived from $\boldsymbol{t}_1$ first by removing $t_{1,1}$ and inserting ν to get $\boldsymbol{t}'_1$ and then by removing ν and inserting τ_2. This means that $\boldsymbol{t}'_2 = R(\boldsymbol{t}_1, \tau_2, s'_2) = \boldsymbol{t}_2$, and so again we complete the process by putting $\boldsymbol{t}'_i = \boldsymbol{t}_i$ for $i = 3, \dots, n$. There is no conflict with the last condition in the lemma because $\nu \neq \tau_i$ for all i since $\nu \leqslant t_{i,1}$.

[6] T. Dokken, T. Lyche, V. Skytt and K.F. Pettersen, Method for local refinement of geometric or physical representation, Patent application: US-2012-0191423-A1 and PCT/NO10/00317, Filed August 26, 2010. US provision patent application submitted August 26, 2009.

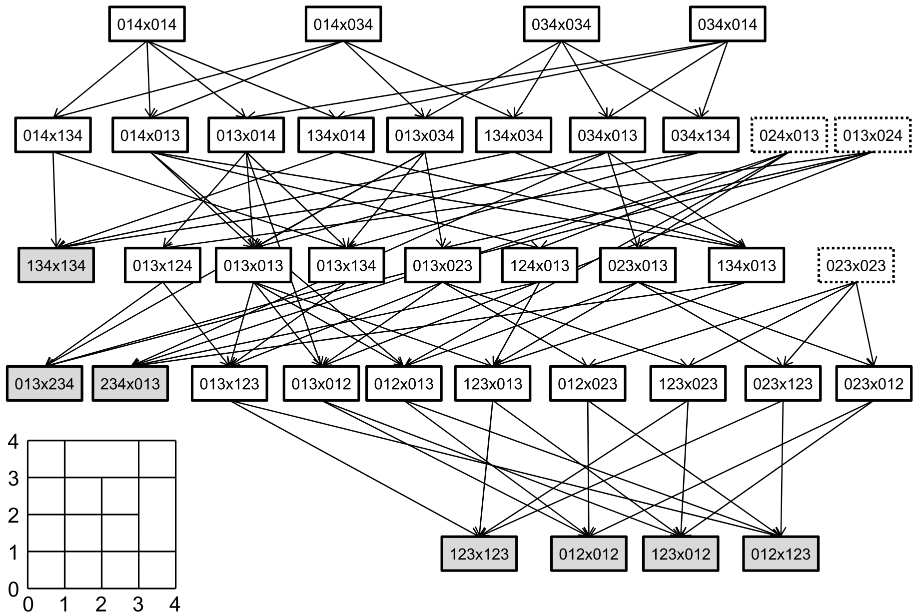

Fig. 18. An LR-mesh and corresponding bilinear LR-graph.

Case 4, both $\tau_2 < \nu$ and $\tau_2 \leqslant t_{1,2}$. This covers all situations that are not under cases 1, 2 or 3. We have $t_{2,1} = \tau_2 < \nu < t_{1,p+2} = t_{2,p+2}$, so just as for case 1, we can use the induction to get the sequence $B_{\boldsymbol{t}'_2}, \dots, B_{\boldsymbol{t}'_n}$ where $\boldsymbol{t}'_2 = R(\boldsymbol{t}_2, \nu, \sigma')$ for some $\sigma' \in \{1, 2\}$. We let $\sigma = \sigma'$ and put $\boldsymbol{t}'_1 := R(\boldsymbol{t}_1, \nu, \sigma)$. If $\sigma' = 1$ then $\boldsymbol{t}'_2$ is derived from $\boldsymbol{t}_1$ by removing $t_{1,1}$ and $t_{1,p+2}$ and inserting τ_2 and ν, while $\boldsymbol{t}'_1$ is derived from $\boldsymbol{t}_1$ by removing $t_{1,p+2}$ and inserting ν. With $s'_2 = 2$ we get $\boldsymbol{t}'_2 = R(\boldsymbol{t}'_1, \tau_2, s'_2)$. On the other hand, if $\sigma' = 2$, then $\boldsymbol{t}'_2$ is derived from $\boldsymbol{t}_2$ by removing τ_2 and inserting ν, then $\boldsymbol{t}'_2 = \boldsymbol{t}'_1$. In either case we have extended to the desired sequence $B_{\boldsymbol{t}'_1}, \dots, B_{\boldsymbol{t}'_n}$, and we are done. $\square$

Before the second lemma, we notice that the process of constructing the LR B-splines can be presented in a graph. Given a d-dimensional mesh $\mathcal{M}$, and $\boldsymbol{p} = (p_1, \dots, p_d)$, and recall the notation (4) for the knot specifications corresponding to knot insertion. We define a directed graph $\mathcal{G}(\mathcal{M}, \boldsymbol{p})$ where the nodes are all the d-variate B-splines $B = B_{\boldsymbol{J}}$ of fixed degree $\boldsymbol{p}$ with support in $\mathcal{M}$, and where there is an edge from $B_{\boldsymbol{J}}$ to $B_{\boldsymbol{J}'}$ whenever $\boldsymbol{J}' = R_k(\boldsymbol{J}, m, s)$ for some k, m, s (clearly, if such an edge exists for $s = 1$ then there is also an edge for the same k and m when $s = 2$, and vice versa). We then say that m splits B (or $\boldsymbol{J}$) in the kth direction. The **sinks** (nodes with no outgoing edge) are the B-splines with minimal support in $\mathcal{M}$. An example of a graph $\mathcal{G}(\mathcal{M}, \boldsymbol{p})$ for a two-dimensional mesh $\mathcal{M}$ and degrees $\boldsymbol{p} = (1, 1)$ is shown in Fig. 18. There are 37 bilinear tensor-product B-splines that can be defined on the mesh shown in this figure. In this graph the nodes are ordered from top to bottom according to the number of missing indices in the knot specifications. There are four missing indices in the top row and no missing indices in the bottom row. The knot specifications of the 7 final minimal support B-splines are shown in gray, while the dotted boxed give knot specifications that are not given initially or not the result of a knot insertion.

Lemma A.3. *Given a d-dimensional mesh $\mathcal{M}$, a multidegree $\boldsymbol{p} = (p_1, \dots, p_d)$, and a path from a node B to a sink node B' on $\mathcal{G}(\mathcal{M}, \boldsymbol{p})$. Also suppose ν splits B in the kth direction for some ν and k. Then we can pick $\sigma \in \{1, 2\}$, such that there exists a path from $B_{R_k(\boldsymbol{T}, \nu, \sigma)}$ to B' on $\mathcal{G}(\mathcal{M}, \boldsymbol{p})$.*

Proof. The path from B to B' is given as

$$B = B_{\boldsymbol{T}_1} \to \dots \to B_{\boldsymbol{T}_N} = B' \tag{A.1}$$

where $\boldsymbol{T}_i = (\boldsymbol{t}_{i,1}, \dots, \boldsymbol{t}_{i,d}) = R_{k_i}(\boldsymbol{T}_{i-1}, \tau_i, s_i)$ for $i = 2, \dots, N$. Set $a_1 = 1$ and let $a_2 < \dots < a_n$ be all the $a \geqslant 2$ such that $k_a = k$. Then $\boldsymbol{t}_{a_i,k} = \boldsymbol{t}_{a_i+1,k} = \dots = \boldsymbol{t}_{a_{i+1}-1,k}$ (or up to $\boldsymbol{t}_{N,k}$ for $i = n$), while $\boldsymbol{t}_{a_i,k} = R(\boldsymbol{t}_{a_{i-1},k}, \tau_{a_i}, s_{a_i})$ for $i = 2, \dots, n$. We can now use Lemma A.2 on the sequences $(B_{\boldsymbol{t}_{a_1,k}}, \dots, B_{\boldsymbol{t}_{a_n,k}})$, $(\tau_{a_2}, \dots, \tau_{a_n})$ and $(s_{a_2}, \dots, s_{a_n})$, and the number ν, giving a new sequence $B_{\boldsymbol{t}'_1}, \dots, B_{\boldsymbol{t}'_n}$ of univariate p_k-degree splines.

We lift this to a sequence $B_{\boldsymbol{T}'_1}, \dots, B_{\boldsymbol{T}'_N}$ where

$$\boldsymbol{T}'_i = \left(\boldsymbol{T}_{i,1}, \dots, \boldsymbol{T}_{i,k-1}, \boldsymbol{t}'_l, \boldsymbol{T}_{i,k+1}, \dots, \boldsymbol{T}_{i,d}\right) \tag{A.2}$$

where l is the biggest l such that $a_l \leqslant i$. We want to show that this sequence is the path we are looking for.

When $k_i \neq k$, we have $\boldsymbol{T}'_i = R_{k_i}(\boldsymbol{T}'_{i-1}, \tau_i, s_i)$. When $k_i = k$ then $i = a_{i'}$ for some i'. Then either $\boldsymbol{t}'_{i'} = \boldsymbol{t}'_{i'-1}$ or $\boldsymbol{t}'_{i'} = R(\boldsymbol{t}'_{i'-1}, \tau_{a_{i'}}, s'_i)$, giving $\boldsymbol{T}'_i = \boldsymbol{T}'_{i-1}$ or $\boldsymbol{T}'_i = R_k(\boldsymbol{T}'_{i-1}, \tau_{a_{i'}}, s'_i)$. Therefore there is a path from $(B_{\boldsymbol{T}'_1})$ to $(B_{\boldsymbol{T}'_N})$ on $\mathcal{G}(\mathcal{M}, \boldsymbol{p})$. From Lemma A.2, there is a $\sigma = 1$ or 2 such that $\boldsymbol{t}'_1 = R(\boldsymbol{t}_{1,k}, \nu, \sigma)$, then $\boldsymbol{T}'_1 = R_k(\boldsymbol{T}, \nu, \sigma)$. The multivariate knot specifications $\boldsymbol{T}'_N$ and $\boldsymbol{T}_N$, are equal on the other parameter directions than the kth, while $T_{N,k}$ includes $T'_{N,k}$. If a knot has higher multiplicity in $\boldsymbol{T}'_{N,k}$ than in $\boldsymbol{T}_{N,k}$, this knot would split $\boldsymbol{T}_N$ in the kth direction, contradicting the fact that B' is a sink. Therefore $\boldsymbol{T}'_N = \boldsymbol{T}_N$, and so $B_{\boldsymbol{T}'_N} = B'$ completing the proof. □

For a collection C of nodes on a directed graph, we let $S(C)$ be the set of all sink nodes N on the graph such that there is a path from a node in C to N.

Proof of Theorem 3.4. Let $\mathcal{M}$ be the final mesh after all insertions, and $\boldsymbol{p}$ be the multi-degree of the B-splines used. Let the sequence $\mathcal{B}_1, \ldots, \mathcal{B}_n$ be the collections of tensor-product B-splines at each step in the refinement process. Hence, $\mathcal{B}_1$ is the set of classical minimal support tensor-product B-splines on the starting tensor mesh, $\mathcal{B}_n$ is a set of minimal support tensor-product meshes on $\mathcal{M}$, and for every step $i = 2, \ldots, n$,

$$\mathcal{B}_i = \left(\mathcal{B}_{i-1} \setminus \{B_{\boldsymbol{J}_i}\}\right) \cup \{B_{R_{k_i}(\boldsymbol{J}_i, m_i, 1)}, B_{R_{k_i}(\boldsymbol{J}_i, m_i, 2)}\} \tag{A.3}$$

for some $\boldsymbol{J}_i$, k_i and m_i such that m_i splits $\boldsymbol{J}_i$ in the k_ith direction. To prove the theorem, we need to show that $\mathcal{B}_n$ only depends on $\mathcal{B}_1$ and the mesh $\mathcal{M}$, and not the intermediate sets $\mathcal{B}_i$ for $i = 2, \ldots, n-1$.

The $\mathcal{B}_i$ can be regarded as sets of nodes on $\mathcal{G}(\mathcal{M}, \boldsymbol{p})$. In that context we can show that $S(\mathcal{B}_{i-1}) = S(\mathcal{B}_i)$ for $i = 2, \ldots, n$ because clearly $S(\mathcal{B}_i) \subset S(\mathcal{B}_{i-1})$, while inclusion the other way follows from Lemma A.3. This gives $S(\mathcal{B}_1) = S(\mathcal{B}_n) = \mathcal{B}_n$ because $\mathcal{B}_n$ only has sink nodes. □

Appendix B. LR B-splines form a nonnegative partition of unity

Proof of Lemma 7.1. There are 4 cases.

1. $B_1, B_2 \notin \tilde{\mathcal{B}}_k$. Since $\tilde{\mathcal{B}}_{k+1} = (\tilde{\mathcal{B}}_k \setminus \{B_0\}) \cup \{B_1, B_2\}$ we find
$$\sum_{B \in \tilde{\mathcal{B}}_{k+1}} \gamma_{k+1,B} B = \sum_{B \in \tilde{\mathcal{B}}_k \setminus \{B_0\}} \gamma_{k,B} B + \gamma_{k,B_0}\alpha_1 B_1 + \gamma_{k,B_0}\alpha_2 B_2. \tag{B.1}$$
Using (43) this reduces to $\sum_{B \in \tilde{\mathcal{B}}_k} \gamma_{k,B} B = 1$.
2. $B_1 \notin \tilde{\mathcal{B}}_k$, $B_2 \in \tilde{\mathcal{B}}_k$. In this case
$$\sum_{B \in \tilde{\mathcal{B}}_{k+1}} \gamma_{k+1,B} B = \sum_{B \in \tilde{\mathcal{B}}_k \setminus \{B_0, B_1\}} \gamma_{k,B} B + \gamma_{k,B_0}\alpha_1 B_1 + (\gamma_{k,B_2} + \gamma_{k,B_0}\alpha_2) B_2.$$
Again using (43) this reduces to $\sum_{B \in \tilde{\mathcal{B}}_k} \gamma_{k,B} B = 1$.
3. $B_1 \in \tilde{\mathcal{B}}_k$, $B_2 \notin \tilde{\mathcal{B}}_k$. This is similar to the previous case.
4. $B_1, B_2 \in \tilde{\mathcal{B}}_k$. Now $\tilde{\mathcal{B}}_{k+1} = \tilde{\mathcal{B}}_k \setminus \{B_0\}$ and
$$\begin{aligned}\sum_{B \in \tilde{\mathcal{B}}_{k+1}} \gamma_{k+1,B} B &= \sum_{B \in \tilde{\mathcal{B}}_k \setminus \{B_0, B_1, B_2\}} \gamma_{k,B} B + (\gamma_{k,B_1} + \gamma_{k,B_0}\alpha_1) B_1 + (\gamma_{k,B_2} + \gamma_{k,B_0}\alpha_2) B_2 \\ &= \sum_{B \in \tilde{\mathcal{B}}_k} \gamma_{k,B} B = 1.\end{aligned}$$

This proves (44). Clearly (45) follows for $B \in \tilde{\mathcal{B}}_{k+1} \setminus \{B_0, B_1, B_2\}$. For $B_l \notin \tilde{\mathcal{B}}_k$ we have $c_{k+1,B_l} = c_{k,B_0}$, while for $B_l \in \tilde{\mathcal{B}}_k$ we get c_{k+1,B_l} if we add a contribution to c_{k,B_l}, and rescale.

It remains to prove that $\gamma_{k+1,B}$ is positive. There are three cases:

- $\gamma_{k+1,B} = \gamma_{k,B}$, if $K \in \tilde{\mathcal{B}}_k \setminus \{B_0, B_1, B_2\}$. In this case the weight is left unchanged, so the new weight is positive.
- $\gamma_{k+1,B} = \gamma_{k,B_0}\alpha_l$, if $B = B_l \notin \tilde{\mathcal{B}}_k$, $l = 1, 2$. As it is assumed that the B-spline corresponding to B_0 does not have minimal support in the mesh corresponding to $\tilde{\mathcal{B}}_{k+1}$, the knot value is inserted between the first and last knot value of B_0. From (8) it follows that $\alpha_l > 0$, and that $\gamma_{k+1,B}$ is positive as it is the product of two positive numbers.
- $\gamma_{k+1,B} = \gamma_{k,B} + \gamma_{k,B_0}\alpha_l$, if $B = B_l \in \tilde{\mathcal{B}}_k$, $l = 1, 2$. In this case we add $\gamma_{k,B_0}\alpha_l$, that is proved positive above, to the old weight that is positive, ensuring that $\gamma_{k+1,B}$ is positive. □

References

Buffa, A., Cho, D., Sangalli, G., 2010. Linear independence of the T-spline blending functions associated with some particular T-meshes. Comput. Methods Appl. Mech. Engrg. 199 (23–24), 1437–1445.

Babenko, Y., Leskevich, T., Mirebeau, J.-M., 2011. Sharp asymptotics of the Lp approximation error for interpolation on block partitions. Numer. Math. 117, 397–423.

Bazilevs, Y., Calo, V.M., Cottrell, J.A., Evans, J.A., Hughes, T.J.R., Lipton, S., Scott, M.A., Sederberg, T.W., 2010. Isogeometric analysis using T-splines. Comput. Methods Appl. Mech. Engrg. 199 (5–8), 229–263.

Cottrell, J.A., Hughes, T.J.R., Bazilevs, Y., 2009. Isogeometric Analysis: Toward Integration of CAD and FEA. John Wiley & Sons, Chichester.

Deng, J., Chen, F., Li, X., Hu, C., Tong, W., Yang, Z., Feng, Y., 2008. Polynomial splines over hierarchical T-meshes. Graph. Models 70, 76–86.

Dokken, T., Skytt, V., Haenisch, J., Bengtsson, K., 2009. Isogeometric representation and analysis: bridging the gap between CAD and analysis. In: 47th AIAA Aerospace Sciences Meeting Including The New Horizons Forum and Aerospace Exposition. 5–8 January 2009, Orlando, Florida. American Institute of Aeronautics and Astronautics.

Forsey, D.R., Bartels, R.H., 1988. Hierarchical B-spline refinement. Comput. Graph. 22, 205–212.

Hughes, T.J.R., Cottrell, J.A., Bazilevs, Y., 2005. Isogeometric analysis: CAD, finite elements, NURBS, exact geometry, and mesh refinement. Comput. Methods Appl. Mech. Engrg. 194, 4135–4195.

Kraft, R., 1998. Adaptive und linear unabhangige multilevel B-splines und ihre Anwendungen. PhD thesis, Math. Inst. A, University of Stuttgart.

Li, X., Chen, F., 2011. On the instability in the dimension of splines spaces over T-meshes. Comput. Aided Geom. Design 28, 420–426.

Mourrain, B., 2010. On the dimension of spline spaces on planar T-subdivisions. Preprint, http://hal.inria.fr/inria-00533187/en.

Pettersen, K.F., 2013. On the dimension of multivariate spline spaces. Report SINTEF A23875, ISBN 9788214053135.

Schumaker, L.L., 2007. Spline Functions: Basis Theory, third edition. Cambridge University Press, Cambridge.

Schumaker, L.L., Wang, L., 2011. Spline spaces on TR-meshes with hanging vertices. Numer. Math. 118, 531–548.

Schumaker, L.L., Wang, L., 2012. Approximation power of polynomial splines on T-mesh. Comput. Aided Geom. Design 29, 599–612.

Scott, M.A., Li, X., Sederberg, T.W., Hughes, T.J.R., 2011. Local refinement of analysis-suitable T-splines. Comput. Methods Appl. Mech. Engrg. 213–216, 206–222.

Sederberg, T.W., Zheng, J., Bakenov, A., Nasri, A., 2003. T-splines and T-NURCCS. ACM Trans. Graph. 22, 477–484.

Sederberg, T.W., Cardon, D.L., Finnigan, G.T., North, N.S., Zheng, J., Lyche, T., 2004. T-spline simplification and local refinement. ACM Trans. Graph. 23, 276–283.

Vuong, A.V., Giannelli, C., Jüttler, B., Simeon, B., 2011. A hierarchical approach to adaptive local refinement in isogeometric analysis. Comput. Methods Appl. Mech. Engrg. 200, 3554–3567.